Energy, Mines and Resources Canada | Énergie, Mines et Ressources Canada

CANMET

Canada Centre for Mineral and Energy Technology | Centre canadien de la technologie des minéraux et de l'énergie

SOLUBILITY OF LEAD CHLORIDE IN FERRIC CHLORIDE LEACHING MEDIA

K. Bartels, P.L. Bedard and K.G. Tan
Metallurgical Chemistry Section
Extractive Metallurgy Laboratory

November 1985

Project: MRP-3.0.52.07
Chloride Processes for Sulphide Ore Treatment

This document is an unedited ... (CANMET)

Ce document est un rapport ... (CANMET)

107 pp

MINERALS RESEARCH PROGRAM
MINERAL SCIENCES LABORATORIES
DIVISION REPORT MRP/MSL 85-7 (TR)

MICROMEDIA
MAR 3 1986

Crown Copyrights Reserved

SOLUBILITY OF LEAD CHLORIDE IN FERRIC CHLORIDE LEACHING MEDIA

by

K. Bartels*, P.L. Bedard** and K.G. Tan***

ABSTRACT

The solubilities of $PbCl_2$ in various $FeCl_3$ - $FeCl_2$ - HCl leaching media and the densities of the corresponding $PbCl_2$-saturated solutions have been measured, using a pycnometric sampling method, over the temperature range 20-100°C for aqueous systems containing: (a) $PbCl_2$ and HCl; (b) $PbCl_2$, $FeCl_3$ and HCl; (c) $PbCl_2$, HCl, $FeCl_3$ and $FeCl_2$; (d) $PbCl_2$, HCl, $FeCl_3$ and $MgCl_2$; (e) $PbCl_2$ and NaCl; and (f) $PbCl_2$, HCl and NaCl.

The measured solubility and density data were fitted to a selection of parametric equations. The observed values and their respective parameters are presented in tabular and graphical form. In addition, three-dimensional solubility 'surfaces' have been generated that illustrate the overall solubility of $PbCl_2$ in several pseudo-binary systems.

---

* Chemist, ** Research Technician, and *** Research Scientist, Metallurgical Chemistry Section, Mineral Sciences Laboratories, CANMET, Energy, Mines and Resources, Canada, 555 Booth Street, Ottawa, Ontario K1A 0G1.

SOLUBILITÉ DU CHLORURE DE PLOMB DANS DES SOLUTIONS DE LIXIVIATION DE CHLORURE FERRIQUE

par

K. Bartels*, P.L. Bedard** et K.G. Tan***

RÉSUMÉ

On a mesuré à l'aide d'une méthode pycnométrique d'échantillonnage la solubilité du $PbCl_2$ dans plusieurs solutions de lixiviation $FeCl_3$, $FeCl_2$, HCl ainsi que la densité des solutions saturées $PbCl_2$ correspondantes, dans un intervalle de températures allant de 20° à 100°C pour les systèmes aqueux contenant: a) $PbCl_2$ et HCl; b) $PbCl_2$, $FeCl_3$ et HCl; c) $PbCl_2$, HCl, $FeCl_3$ et $FeCl_2$; d) $PbCl_2$, HCl, $FeCl_3$ et $MgCl_2$; e) $PbCl_2$ et NaCl; et f) $PbCl_2$, HCl et NaCl.

Les données obtenues des mesures de la solubilité et de la densité ont été ajustées à des équations paramétriques choisies. Les valeurs observées et leurs paramètres respectifs sont présentés sous forme de tableaux et de graphiques. De plus, des "surfaces" de solubilité à trois dimensions ont été produites, illustrant la solubilité complète du $PbCl_2$ dans plusieurs systèmes pseudo-binaires.

---

*Chimiste, **Technicien chercheur, ***Chercheur scientifique, Section de la chimie métallurgique, Laboratoires des sciences minérales, CANMET, Énergie, Mines et Ressources Canada, 555, rue Booth, Ottawa (Ontario) K1A 0G1.

INTRODUCTION

CANMET's ferric chloride leach process for the treatment of complex sulphide bulk concentrates (1) takes advantage of excellent leach kinetics at atmospheric pressure, good selectivity, and potential silver and elemental sulphur by-product recoveries. Since lead is present in significant amounts in these concentrates (typical analysis: 28% Zn, 9% Pb, 0.8% Cu, 19% Fe and 35% S), and as the process may also be of interest for the hydrometallurgical treatment of lead concentrates, the limited lead solubility in the leaching medium determines the maximum process pulp density.

A high grade intermediate product is produced by crystallization of $PbCl_2$ from the leach solution at a suitably low temperature. Lead metal can be recovered electrolytically from the $PbCl_2$ product, either from fused salt or aqueous chloride solutions; both processes generate Cl_2 at the anode. The chlorine is used to regenerate the lixiviant by oxidizing the ferrous chloride, and the process as a whole is largely self sustaining, requiring only minor reagent make-up and bleed streams.

To optimize the leaching and crystallization sections the solubility of $PbCl_2$ is required as a function of temperature and of the concentrations of $FeCl_3$, $FeCl_2$, HCl and NaCl. Besides the $FeCl_3$ lixiviant that is reduced to $FeCl_2$ during the leach, some HCl is needed to prevent hydrolysis, and up to 3.0 M NaCl can be added to improve the lead and silver solubilities. Some calcium chloride may also be present to control the soluble sulphate level. The present study was undertaken to provide the necessary $PbCl_2$ solubility data for process design; $MgCl_2$ additions served to explore the effect of the presence of chloride co-electrolytes other than those already mentioned. A similar study on the solubility of AgCl in various chloride leach media was recently reported (2).

The extensive solubility and density data for the $PbCl_2$-H_2O system in the open literature were compiled and reviewed (3). For temperatures ranging from 0 to 100°C, the $PbCl_2$ solubility (S) in water and the densities of the corresponding saturated solutions (d) were best represented by quadratic equations:

$$S = 0.000131t^2 + 0.0133t + 0.657 \quad (g/100\ g\ solution) \qquad (1)$$

$$d = -0.0025t^2 + 0.05t + 1007 \quad (g/L) \qquad (2)$$

Although solubility data of $PbCl_2$ in many binary and some ternary chloride systems are available (3), no specific solubility or density data for aqueous $FeCl_3/FeCl_2$-HCl systems have been reported. Preliminary tests in aqueous $FeCl_3$-HCl and $FeCl_2$-HCl systems at 100°C (4) indicated that the effects of ferric chloride additions might not be straightforward. Whereas the $PbCl_2$ solubility in the $FeCl_2$-HCl system increased monotonically and significantly with the total chloride concentration, the $PbCl_2$ solubility in the $FeCl_3$-HCl system increased only slightly with $FeCl_3$ concentration, and a minimum was observed at 0.3 M HCl for $FeCl_3$ concentrations held constant in the range of 0.5 M to 2.5 M.

Clever and Johnston (5) evaluated the solubility of various lead salts reported in the literature and commented on the fundamental and practical considerations of different solubility measurement methods. For $PbCl_2$-H_2O they quote similar values to Bartels' (3); for aqueous chloride-perchlorate electrolytes the results of Nriagu and Anderson (6), Mironov (7) and Fedorov (8) are discussed in detail.

The purpose of the present study was to obtain $PbCl_2$ solubility data in aqueous $FeCl_3$ - $FeCl_2$ - HCl solutions with co-electrolyte concentrations ranging up to the high levels of interest to the hydrometallurgical industry (1). To provide a complete overview and more insight into the fundamental

solubility relationships, a systematic variation of the solution components and their individual concentrations was undertaken between 20 and 100°C. The measured solubilities and solution densities were fitted to parametric equations, and the results are discussed in qualitative terms.

FUNDAMENTALS

A convenient description of lead chloride solutions in aqueous chloride media (5,6) is based on the dissociation and complex formation equilibria according to:

$$PbCl_2(s) = PbCl_2(aq) \quad (3)$$

$$PbCl_2(aq) = Pb^{2+} + 2Cl^- \quad (4)$$

$$PbCl_2(aq) = PbCl^+ + Cl^- \quad (5)$$

$$PbCl_2(aq) + Cl^- = PbCl_3^- \quad (6)$$

$$PbCl_2(aq) + 2Cl^- = PbCl_4^{2-} \quad (7)$$

Consideration of the associated equilibrium constants predicted the general form of the solubility isotherms to be:

$$S_t = A/c^2 + B/c + Cc^2 + Dc + E \text{ (g/L soln)} \quad (8)$$

where S_t (g/L) is the amount of $PbCl_2$ contained in a solution of c (g/L) of the chloride component at temperature t (°C). Although the equation was derived for molar concentrations of $PbCl_2$ and free Cl^- in the $PbCl_2$-H_2O system only, the polynomial is particularly useful for fitting solubility data in more complicated systems. It effectively encompasses both the reduction in $PbCl_2$ solubility due to the common ion effect in the first two terms (i.e., by the magnitude of the constants A and B), and the $PbCl_2$ solubility increases due to the formation of anionic complexes at high Cl^- concentrations. It should be noted, however, that at low values of c, the

first two terms tend to infinity, and data for total Cl^- concentrations less than 0.1 M are subject to large errors.

The solubility of $PbCl_2$ always increases with temperature, reflecting the endothermic heat of solution. The measured data are expected to obey the integrated form of the van't Hoff equation (2):

$$\Delta H_{soln} = -19.13 \times d(\log s)/d(1000/T) \quad > 0 \quad (kJ/mol) \qquad (9)$$

Hence, the temperature dependence of the $PbCl_2$ solubility in a particular system may be approximated by a straight line with a negative slope:

$$\log s = A \times (1000/T) + B \qquad (10)$$

In practice, a better fit of the solubility data with respect to temperature is obtained by representing the data points by a number of parametric equations that increase monotonically with temperature. Dinardo and Dutrizac (2) adequately fitted the AgCl solubility data with a quadratic equation: $S = A + Bt + Ct^2$. For $PbCl_2$ solubilities, however, a more flexible exponential polynomial was used:

$$S = At \times e^{Bt} + C \qquad (11)$$

This equation is particularly well suited for describing curves with linear attributes at low t and more pronounced exponential behaviour at high t.

Isothermal solution densities generally display a linear increase with the amount of the dissolved solute (3,9). The temperature dependence of the densities of $PbCl_2$ saturated solutions, especially in the presence of other chlorides, can generally be approximated by a straight line with a negative slope:

$$d = At + B \qquad (12)$$

This linearization of the density curves may be attributed to the partial compensation of the curvilinear density decreases due to thermal expansion by the increased $PbCl_2$ solubilities at higher temperatures and by changes in solution structure brought about by the polarizing effect of the dissolved electrolytes (electrostriction).

Although the experimental results should fit a quantitative model involving the activities of individual dissolved species as calculated from their respective equilibrium constants, such calculations are especially problematic and complex for concentrated brines (10-13). At the present stage, a more qualitative discussion in terms of common ion effects, dissociation equilibria, saturation levels, heats of solution, and density relationships appears to be practical.

The $PbCl_2$ solubility isotherms in chloride media generally display a rather flat minimum at low total Cl^- concentrations (<1 M). The substantial depression of the $PbCl_2$ solubility at these minima compared to pure aqueous solutions is due to the common ion effect. According to the classical solubility product concept, the limitations and implications of which are discussed by Lewin (11), the dissociation of $PbCl_2$ (Equations 4 and 5) is suppressed by small additions of Cl^- from other sources. Larger free Cl^- additions tend to increase the $PbCl_2$ solubility by complex formation and/or induced changes in the activity coefficients. A quantitative theoretical treatment requires the exact and complete definition of all the soluble species and their associated stability constants. In the concentrated solutions of interest in hydrometallurgy, the activity coefficients of the solutes and of the solvent (water) must also be considered. The nature of the solution changes drastically as less water becomes available per mole of electrolyte; ion pairing, polymerization and ionic saturation levels may be observed. In systems containing ferric chloride, in particular, vivid

colour changes are observed on heating and on changing the concentrations of the different solution components. Irregularities of the measured solubility and density curves most frequently occur in highly concentrated brines.

Since the margin for experimental error also increases in these high concentration regions, even with pycnometric methods of solution sampling, a reliable independent consistency check is also required. The straight line behaviour of the density vs. temperature curves was used in the present study, even though it is dominated by the co-electrolyte concentrations and lacks a quantitative theoretical foundation. Nevertheless, preliminary calculations have shown that the application of a linear additivity rule for solution densities, using empirical contribution factors, may be applied. Work is continuing on this particular aspect.

In binary solutions, the heat of solution can be considered as the difference between the endothermic work to overcome the lattice energy and the exothermic heats of hydration of the component ions (12, 13). The calculation of ion-solvent interactions and some applicable solution models are discussed by Bockris and Reddy (13). Qualitatively, the heats of hydration increase with the charge/size ratio of the respective ions. In concentrated brines, however, many additional aspects of the complexed species and ion clusters have to be considered, such as relative heats of formation, hydration numbers, effective charge/size relationships, etc. Experimental results for concentrated binary solutions quoted in reference (13) indicate a linear dependence of the logarithm of the mean activity coefficient on the cube root of the concentration; this may eventually form a basis for the development of a quasi-lattice model.

EXPERIMENTAL

A pycnometric procedure was developed for sampling saturated aqueous solutions in equilibrium with solid $PbCl_2$ (14). Mass-volume calibration data were established for a number of pycnometers over the temperature range 20 to 100°C. Sample solutions were diluted to the appropriate levels for the determination of lead by atomic absorption spectrophotometry.

The $PbCl_2$ solubility data were fitted by means of the 'Simplex' method (15) to the exponential Equation 11. A 'least-squares' fit of the data to the linear logarithmic Equation 10 was also performed, and heats of solution were calculated from the slopes of these lines according to Equation 9. Density data are required for conversion between conventional solubility units; e.g., g/L, molar, molal, percent weight, etc. The linear fit of the density data to Equation 12 also served as a consistency check on the sampling procedure.

The $PbCl_2$ solubility isotherms as a function of the individual co-electrolyte concentrations were approximated by the polynomial Equation 8. The fit obtained with physically meaningful parameters A, B, C, D and E was quite poor in the low concentration region (6), and in the present work the equation was used for curve-fitting purposes only, again by means of the 'Simplex' method. This allowed the construction of three dimensional solubility surfaces for pseudo-binary systems that present a convenient overview of the $PbCl_2$ solubility behaviour. All of the above data are represented in tables and/or graphical form as a basis for discussion.

Reagents

All solution components were of analytical grade and were not subjected to any further purification. The various test solutions were prepared using doubly distilled water.

Apparatus

The apparatus used for the solubility measurements is shown in Figure 1. The reaction vessel is placed in a thermostatted bath of silicone oil. The lid of the reaction vessel and the outside of the silicone oil bath are insulated with glass wool batting. A Haake Model E-3 thermostat is used, in conjunction with a Fisher "Dynamix" stirrer and cooling water flowing through a copper cooling coil, to control the temperature to within +/- 0.1°C. The reaction vessel is fitted with a condenser, a stirring motor, a thermometer and a sampling tube. The sampling tube (Figure 2) contains a glass and plastic covered wire loop for retrieving the pycnometer and is wrapped for 9 cm above the lid of the reaction vessel with a heating tape which is controlled by a variable transformer. The sampling tube is 25 mm in diameter and is fitted with a coarse frit to avoid carry-over of solute particulates when sampling the bulk solution. The pycnometer is constructed from a 7/16 outer tapered joint and a number 9800 Pyrex test tube. The pycnometer is used with two separate capillary tops for the ranges 20-40°C and 40-100°C. Both capillaries are attached to 7/16 standard taper inner joints.

The two capillary tops are shown in Figures 3(a) and 3(b). The shorter top is used for sampling saturated solutions below 40°C, whereas the longer top is used for solutions above 40°C. When sampling at higher temperatures, some cooling takes place before the sample can be weighed. The longer top, with a 7 cm capillary of 0.3 mm bore, is sufficient to limit evaporation, and weighings may be made when the meniscus reaches the point indicated by the 'weight reading line'. This method ensures a consistent weighing procedure with respect to the volume-temperature calibration of the pycnometers.

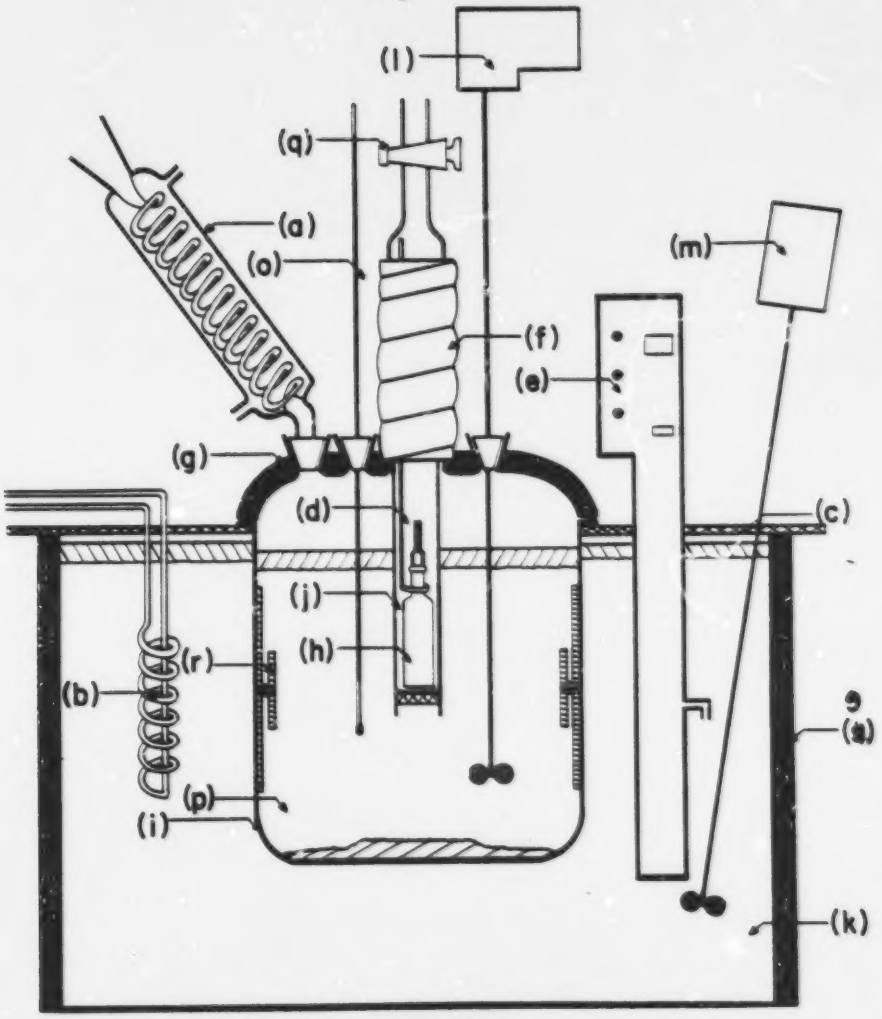

Fig. 1 - Solubility determination apparatus:

(a) Condenser (24/40 ground glass joint)
(b) Cooling water coil (copper)
(c) Cover plate
(d) Glass loop retriever (glass and wire covered with Teflon tape)
(e) Heater-Thermostat (Haake Model E-3)
(f) Heating tape
(g) Insulation (glass wool)
(h) Pycnometer
(i) Reaction vessel (2.0 L)
(j) Sampling tube (34/40 ground glass joint, 25 mm coarse frit)
(k) Silicone oil
(l) Stirrer (Canlab, 24/40 Teflon stopper)
(m) Stirrer (Fisher "Dynamix")
(o) Thermometer (+/- 0.1°C, 24/40 silicone rubber stopper)
(p) Thermostated solution
(q) Stopcock (2 mm straight bore Teflon plug)
(r) Stirring baffles (titanium - used only for the HCl system).

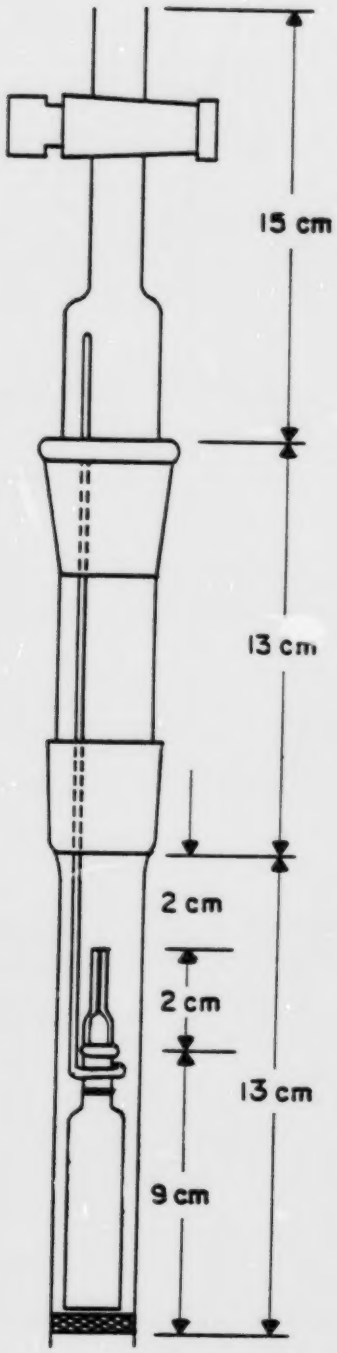

Fig. 2 - Detail of the sampling tube and pycnometer.

Fig. 3(a)

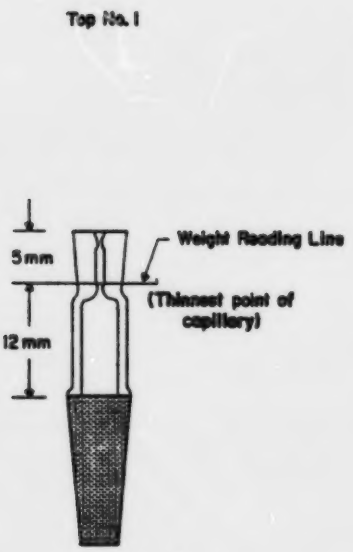

Fig. 3(b)

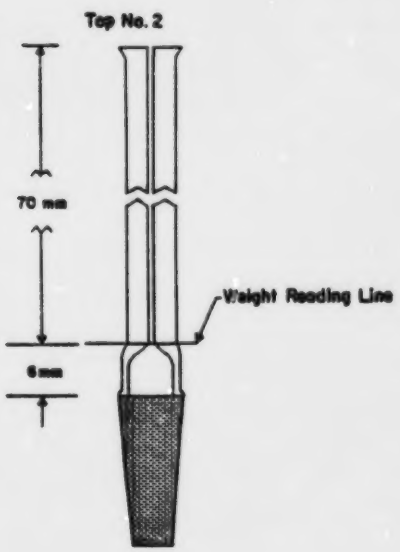

Fig. 3(a) and 3(b) - Low and high temperature pycnometer tops, respectively.

Procedure

Sixty grams of powdered $PbCl_2$ were added to two litres of solution of known composition which were then stirred for at least 2 h at a constant temperature. More $PbCl_2$ was added in 10 g portions when the solubility exceded 30 g/L. A sample of the bulk solution was taken by applying suction from a vacuum pump at the stopcock of the sampling tube. Forceps enclosed in Tygon tubing were used to insert the tops in the pycnometer. To assure complete filling of the capillaries in the pycnometer tops, these were inserted with the level of the sample solution above the opening of the pycnometer. The completely-filled pycnometer and top were then removed using the glass loop. The outside was rinsed with doubly distilled water, dried with a lint-free tissue and weighed on an analytical balance. The weight was taken when the level of the solution in the capillary top had dropped to the "weight reading lines" indicated in Figures 3(a) and 3(b). The contents of the pycnometer were quantitatively transferred into a volumetric flask, and diluted to the mark with distilled water. Subsamples were taken for various analyses, either by titration or atomic absorption spectrophotometry.

After sampling, the excess solution in the sampling tube was returned to the reaction vessel by applying compressed air to the stopcock. The rinsed and dried pycnometer was re-inserted in the sampling tube, and the solution temperature was adjusted by heating or cooling the water bath. The solution was allowed to equilibrate at the new sampling temperature, and the sampling procedure was repeated until sufficient data points in the range of 20 to 100°C were obtained. Saturation curves were measured on both heating and cooling to ensure that equilibrium was actually reached. Data on sample weights, calibrated pycnometer volumes, dilution factors and measured lead concentrations were evaluated using standardized programs.

RESULTS AND DISCUSSION

The effect of the systematic variation of the individual co-electrolyte components on the $PbCl_2$ solubility and on the saturated solution density is reported in separate sections. Details of the experimental results are presented in a standardized tabular and graphical form for all measured systems. Qualitative discussion to illustrate trends and to rationalize the observed behaviour is also provided.

Lead Chloride Solubilities in the Aqueous $PbCl_2$-HCl System

The $PbCl_2$ solubility was measured in aqueous solutions containing 0.1, 0.2, 0.3, 0.7, 1.0, 1.5 and 3.0 M HCl. Table 1 provides the calculated parameters and corresponding correlation coefficients describing the $PbCl_2$-HCl-H_2O system at each HCl concentration. The Table is divided into three sections representing: a) the $PbCl_2$ solubility S in g/L; b) the $PbCl_2$ saturated solution density in g/mL; and c) the logarithm of the $PbCl_2$ solubility s in g/100 g solution.

The family of solubility curves from Table 1a are plotted with the measured data points in Figures 4 and 5. The common ion effect causes a depression of the $PbCl_2$ solubility with increasing HCl additions to 0.7 M HCl (Figure 4). Above 1.0 M HCl the $PbCl_2$ solubility increases due to complex formation (Figure 5). The curves in both figures are quite similar in form (the 0.7 M and 1.0 M curves practically coincide), and the steep monotonic increase of $PbCl_2$ solubility with temperature, reflecting the endothermic heat of solution, is evident in all cases.

The density equations from Table 1b are plotted in Figures 6 and 7, and the straight lines fit the measured data reasonably well in all cases. The density lines for the 0.1, 0.2 and 0.3 M HCl systems in Figure 6 almost

coincide due to the fact that the increased HCl content significantly depresses the $PbCl_2$ solubility in this dilute region (common ion effect). The density lines for 0.7, 1.0 and 1.5 M HCl (Table 1b, Figures 6 and 7) have a steeper negative slope reflecting the depressed $PbCl_2$ solubility at these HCl concentrations. These curves however, are spaced wider apart because of the more significant differences in the HCl contribution to the overall solution density. The 3.0 M HCl line in Figure 7 shows the effect of increases in both the HCl and $PbCl_2$ concentrations. The spacing with respect to the 1.5 M HCl is substantial, and its slope is parallel to the 0.1-0.3 M lines (see Table 1b) because the $PbCl_2$ solubility has increased to about the same level as in 0.2 M to 0.3 M HCl. These largely qualitative considerations indicate the applicability of the linear additivity rule for contributions of solutes to the overall solution density, as mentioned in the Fundamentals section.

The integrated van't Hoff equations in Table 1c are plotted in Figures 8 and 9, and with the exception of the 1.5 M HCl system the fit with the measured data points is excellent. The corresponding heats of solution calculated from the slopes of these lines are summarized in Table 2. The magnitudes of the calculated heats of solution are of the right order; i.e., less than +40 kJ/mol (endothermic) for sparingly soluble electrolytes (13). The variations in the heat of solution at different HCl concentrations indicate major changes in the lead chloride complexes present. Although some correlation exists between the $PbCl_2$ solubility and the heat of solution, the observed minima were at 0.3 M HCl for the solubility and at 1.0 M HCl for the heat of solution (most endothermic). It may be that the most drastic changes in the heat of solution are associated with the transition from the common ion effect to the complexation region. This would account for the discrepancy in the location of the above mentioned minima and the larger

deviation of the 1.5 M HCl data from the van't Hoff type behaviour.

The equations in Table 1a were used to generate $PbCl_2$ solubility data for the measured systems (0.1 to 3 M HCl) at discrete temperature intervals. Solubility isotherms as a function of the HCl concentration were fitted to these data according to Equation 8 using a least-squares method, as shown in Table 3 and Figure 10. Best fits were obtained only with physically non-meaningful parameter values (all values in Table 3 should be positive), and disregarding the $PbCl_2$ solubility in pure water (0 M HCl). Figure 10 shows that at all temperatures between 10 and 100°C, the $PbCl_2$ solubility reaches a minimum at about 0.7 M HCl (25 g/L) due to the common ion effect. Further additions of HCl slightly increase the PbCl solubility due to complexation, especially at elevated temperatures.

The parametric description of the $PbCl_2$ solubility as a function of HCl concentration and of temperature allowed the construction of a three-dimensional solubility surface, as shown in Figure 11, using a relatively small grid corresponding to intervals of 5°C and 0.1 M HCl. The surface is relatively flat at low temperatures but is more steeply inclined along the temperature axis owing to the large endothermic heats of solution. The variation of the $PbCl_2$ solubility with HCl concentration is especially pronounced at higher temperatures.

Except for measurements at 25°C, relatively few data were found in the literature for the $PbCl_2$ - HCl - H_2O system (16-20). A limited comparison is given in Table 4; with few exceptions the present results are slightly lower (by less than 5%) than those reported in the earlier publications. The results of Kendall and Sloan at 25.2°C (17) are not shown, but excellent agreement between 30 and 60 g/L HCl was obtained. Outside this concentration range the current results are about 20% lower.

Table 1 - Solubility and density data as a function of temperature for the aqueous $PbCl_2$ - HCl system containing 0.1 to 3.0 M HCl.

Conc. HCl (M)	Fitted Equation Parameters A	B	C	Correlation Coefficients
a) Solubility vs Temperature: $S = At \times e^{Bt} + C$				
0.1	0.08444	0.01040	1.5504	0.99729
0.2	0.07590	0.00903	0.4140	0.99973
0.3	0.04813	0.01268	0.2231	0.99764
0.7	0.03355	0.01376	0.1204	0.99930
1.0	0.02436	0.01705	0.2941	0.99946
1.5	0.02657	0.01646	0.3782	0.99714
3.0	0.03975	0.01475	0.7085	0.99833
b) Density vs Temperature: $d = At + B$				
0.1	-0.0002691	1.0106		0.97737
0.2	-0.0003004	1.0116		0.99493
0.3	-0.0003200	1.0127		0.98978
0.7	-0.0003808	1.0192		0.95367
1.0	-0.0003703	1.0256		0.97030
1.5	-0.0003602	1.0334		0.99689
3.0	-0.0002951	1.0582		0.98517
c) Log Solubility vs 1/T: $\text{Log } s = A \times (1000/T) + B$				
0.1	-1.1510	3.4975		0.99592
0.2	-1.2634	3.6984		0.99761
0.3	-1.4589	4.1763		0.99823
0.7	-1.5357	4.2754		0.99677
1.0	-1.5948	4.4222		0.99833
1.5	-1.5564	4.3330		0.99001
3.0	-1.3764	3.9267		0.99698

d = density of saturated solution (g/mL);
S = $PbCl_2$ solubility (g/L); s = $PbCl_2$ solubility (g/100 g solution);
t = temperature (10 to 100°C); T = absolute temperature (K).

Table 2 - Calculated $PbCl_2$ heats of solution in aqueous solutions at different HCl concentrations.

HCl (mol/L)	0.1	0.2	0.3	0.7	1.0	1.5	3.0
$\Delta H_{Sol'n}$ (kJ/mol)	22.1	24.2	28.0	29.5	30.6	29.9	26.4

Table 3 - Solubility data as a function of HCL concentration (g/L) for the aqueous $PbCl_2$ - HCl system at selected temperatures between 10 and 100°C.

Temp. (°C)	Fitted Equation Parameters* A	B	C x 10^5	D x 10^2	E
10	- 4.25	11.69	-6.511	2.148	-0.459
25	- 33.53	26.00	-6.687	2.855	-0.416
40	- 62.27	41.14	-4.945	3.511	-0.047
50	- 79.70	51.16	-2.363	3.836	0.486
60	- 94.57	60.74	1.423	4.066	1.320
70	-105.6	69.48	6.376	4.209	2.528
80	-113.5	77.67	12.04	4.367	4.133
85	-111.4	79.86	15.57	4.328	5.232
90	-109.5	82.27	18.91	4.369	6.423
100	- 98.12	84.95	25.51	4.523	9.326

*see Equation 8: $S_t = A/c^2 + B/c + Cc^2 + Dc + E$ (g/L).

Table 4 - A comparison of the measured solubility data for the aqueous $PbCl_2$ - HCl system with selected literature values.

Conc. HCl	Temp. (°C)	$PbCl_2$ Solubilities		% Diff.	Reference
		Literature	This work		
4.0 g/L	25.0	4.3 g/L	4.2 g/L	-2	Noyes (16)
8.02 "	"	2.5 "	2.5 "	-	"
9.8 "	"	2.1 "	2.1 "	-	"
1.8 "	"	6.7 "	6.5 "	-3	"
3.65 "	"	4.5 "	4.3 "	-4	"
7.29 "	"	2.7 "	2.6 "	-4	"
6.75 "	25.2	2.9 "	2.8 "	-3	von Ende (18)
18.60 "	"	1.5 "	1.4 "	-7	"
37.41 "	"	1.2 "	1.2 "	-	"
74.74 "	"	1.4 "	1.6 "	+14	"
112.3 "	"	2.2 "	2.2 "	-	"
10.0 "	40.0	0.32 "	0.31 "	-3	Bell (20)
10.0 "	55.0	0.55 "	0.50 "	-9	"
10.0 "	80.0	1.2 "	0.95 "	-20	"
3.98 "	50.0	0.92 "	0.95 "	+3	Wilkerson,
37.5 "	50.0	0.35 "	0.33 "	-6	Bathurst &
3.7 "	80.0	1.7 "	1.6 "	-6	Parton (19)
38.0 "	80.0	0.75 "	0.71 "	-5	"

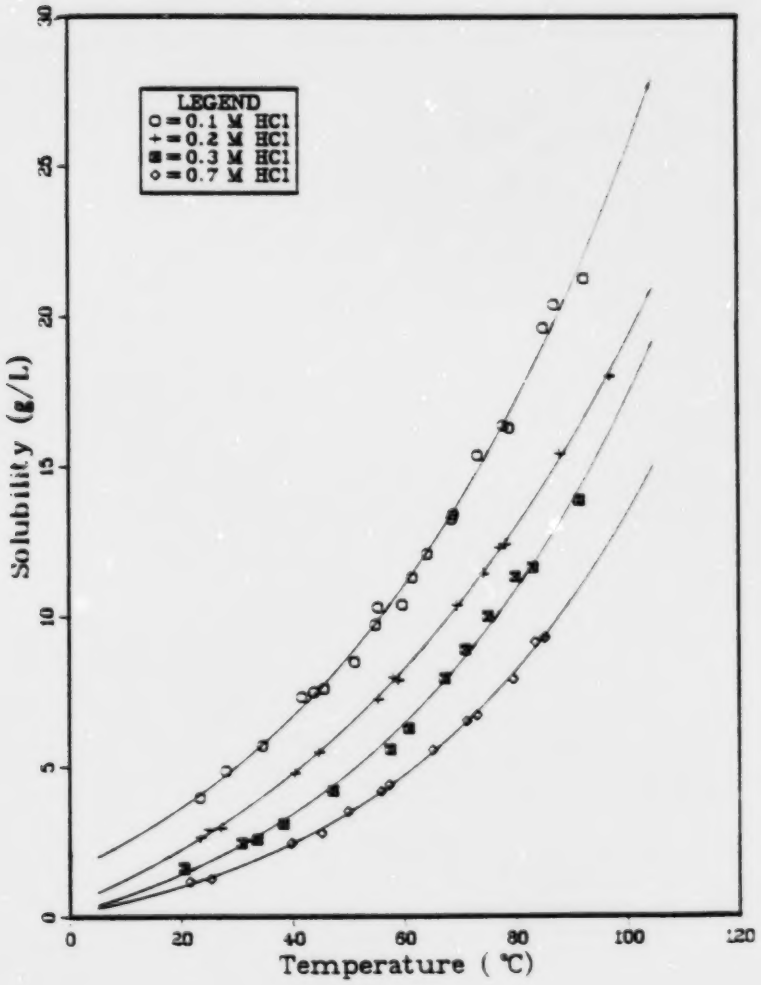

Fig. 4 - Solubility of $PbCl_2$ as a function of temperature for aqueous solutions containing 0.1 to 0.7 M HCl.

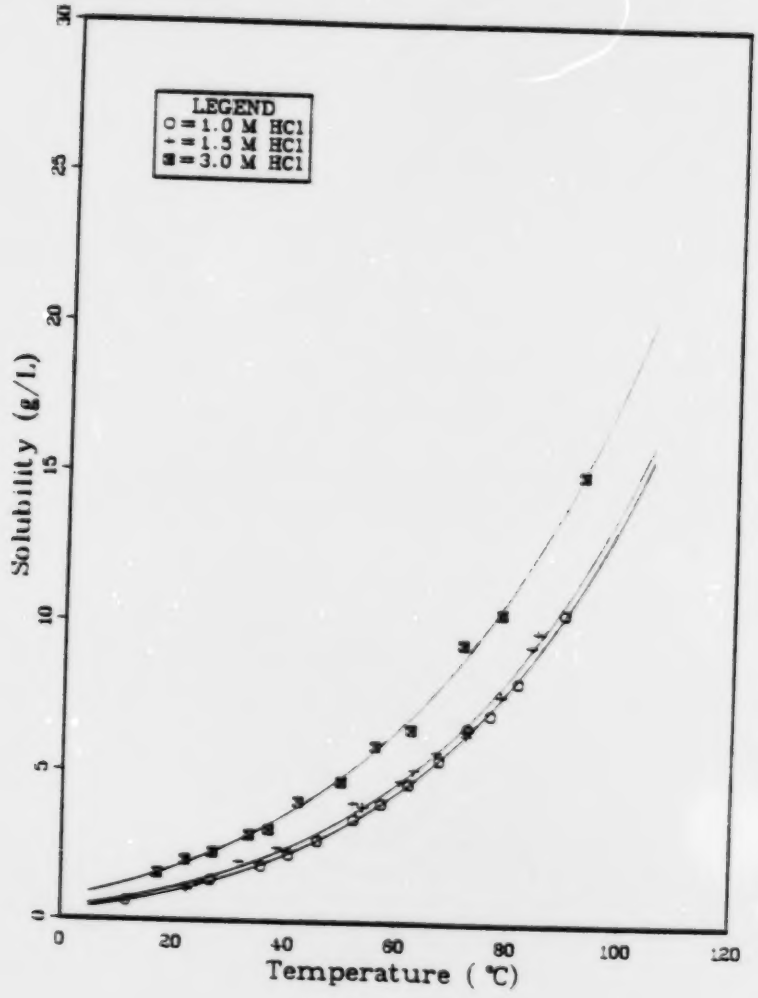

Fig. 5 - Solubility of $PbCl_2$ as a function of temperature for aqueous solutions containing 1.0 to 3.0 M HCl.

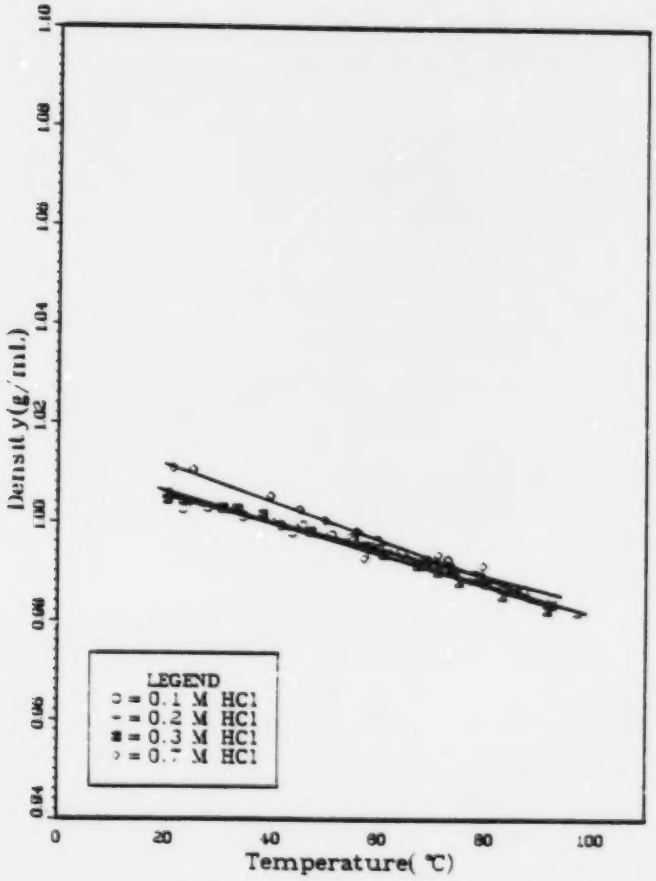

Fig. 6 - Density as a function of temperature for saturated solutions of $PbCl_2$ containing 0.1 to 0.7 M HCl.

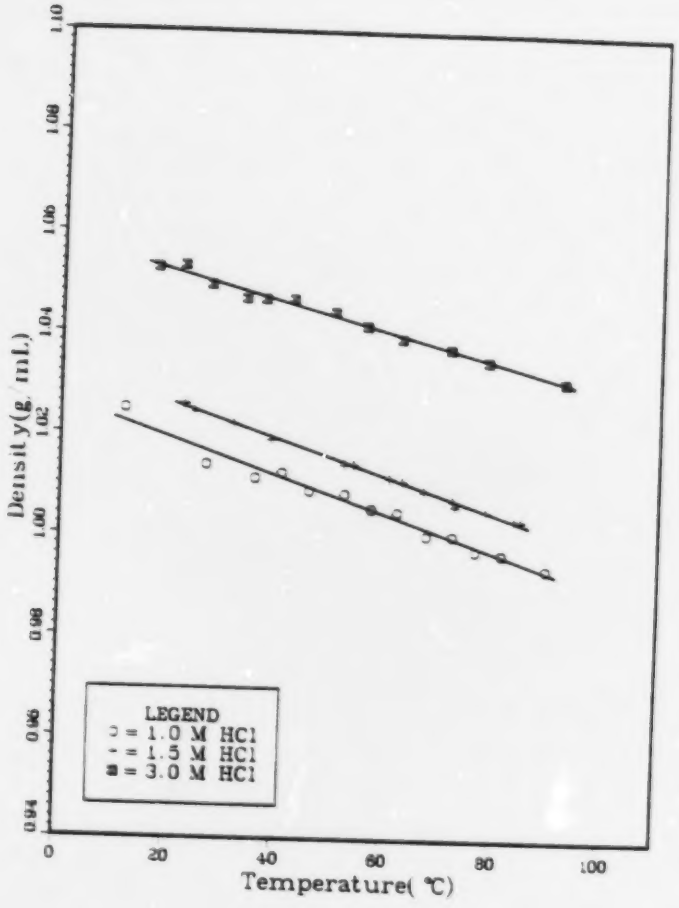

Fig. 7 - Density as a function of temperature for saturated solutions of $PbCl_2$ containing 1.0 to 3.0 M HCl.

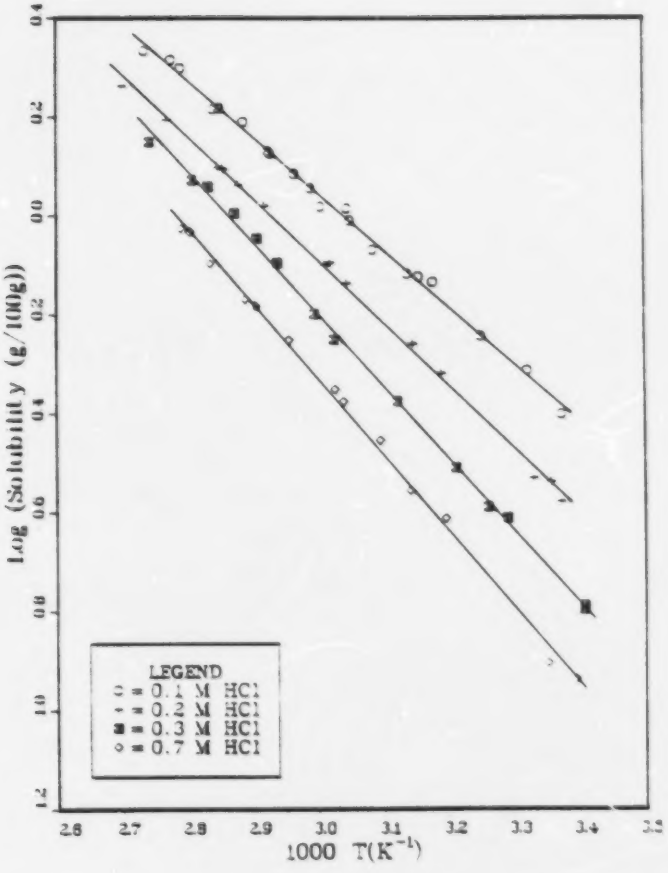

Fig. 8 - The logarithm of the $PbCl_2$ solubility as a function of the reciprocal of the absolute temperature for aqueous solutions containing 0.1 to 0.7 M HCl.

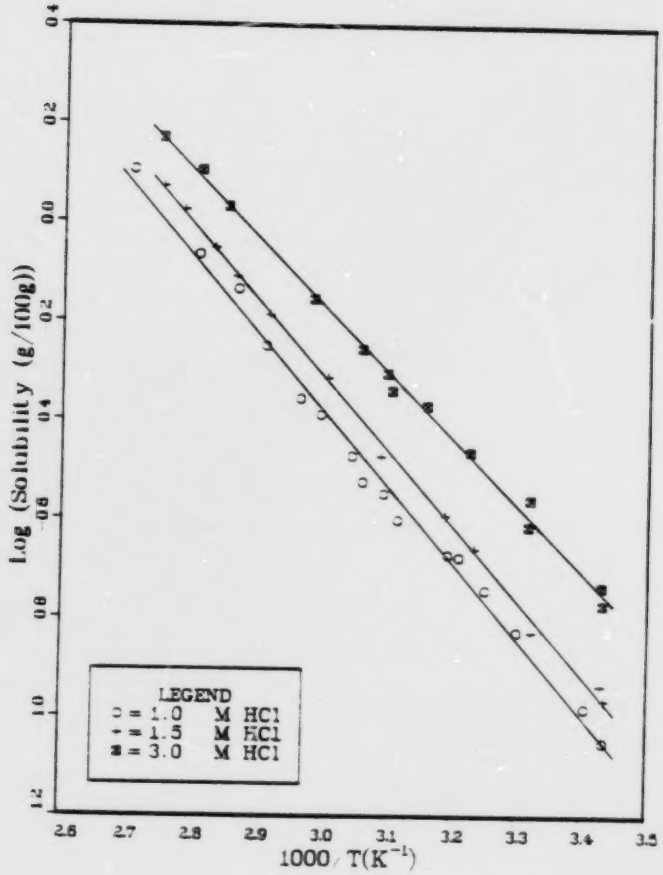

Fig. 9 - The logarithm of the $PbCl_2$ solubility as a function of the reciprocal of the absolute temperature for aqueous solutions containing 1.0 to 3.0 M HCl.

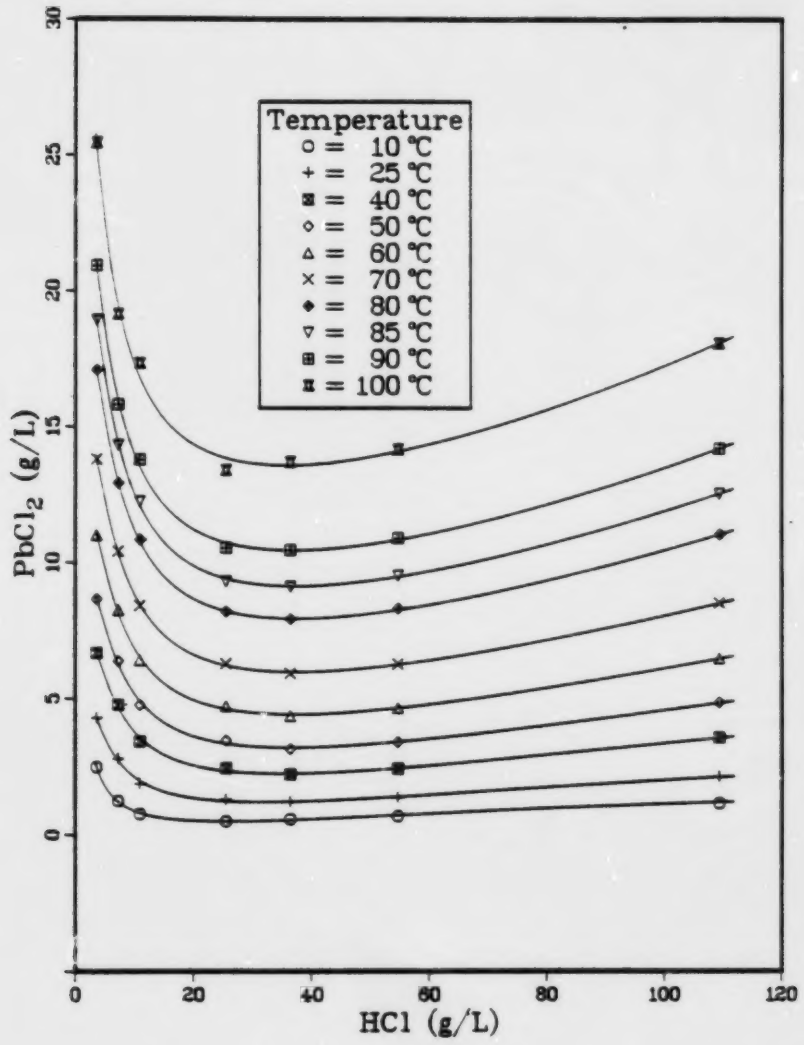

Fig. 10 - Solubility of $PbCl_2$ as a function of HCl concentration for a selected number of temperatures between 10 and 100°C, as obtained from the 'best fit' parameters given in Table 3.

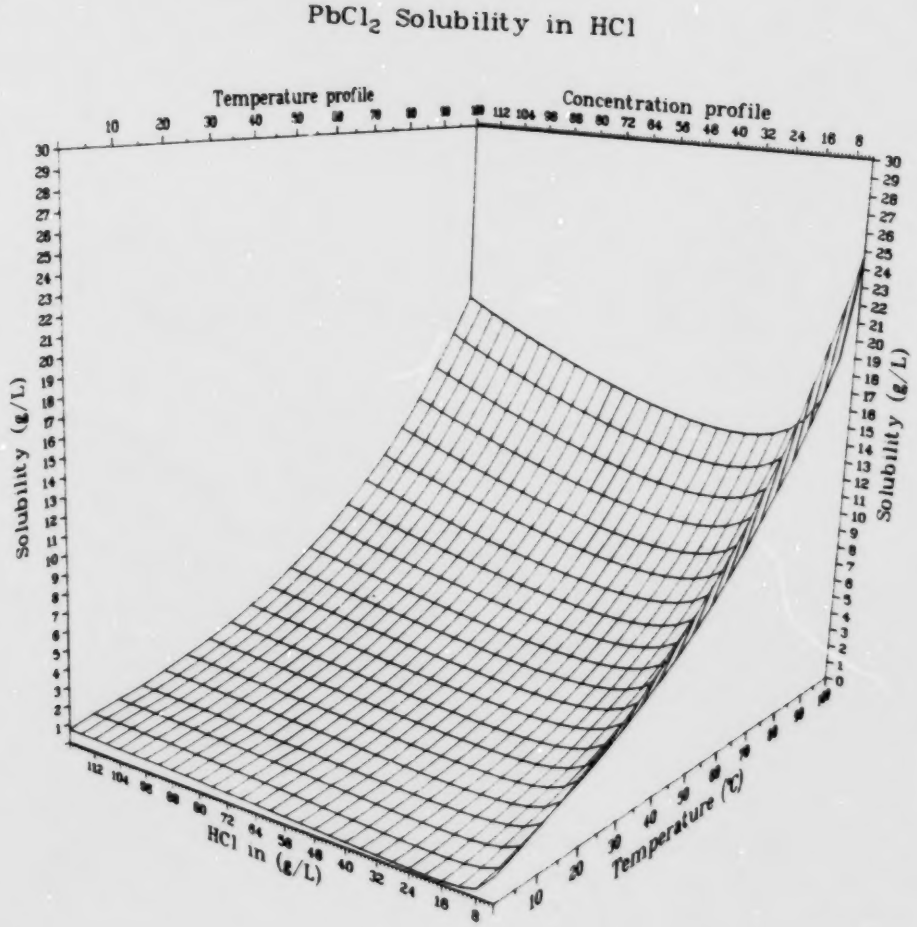

Fig. 11 - The $PbCl_2$ solubility 'surface' as a function of HCl concentration and temperature.

Lead Chloride Solubilities in the Presence of Iron Chlorides and HCl

The addition of iron chlorides to aqueous HCl solutions can either contribute or withdraw free Cl^- ions depending on the predominant iron species in solution. Ferric chloride has a strong tendency for complexation and is expected to withdraw free Cl^- ions, especially at high total chloride concentrations. Ferrous chloride, on the other hand, is expected to act in a more neutral manner or even to augment the free Cl^- concentration by dissociation.

a) The Aqueous $PbCl_2$ - 0.1 M $FeCl_3$ - HCl System

This section reports saturated $PbCl_2$ concentrations in solutions containing 0.1 M $FeCl_3$ and 0.1, 0.175, 0.3, 0.55, 1.0, 2.0 and 3.0 M HCl. Results of the solubility measurements for this system are given in Figures 12 and 13. The corresponding densities of the saturated solutions are presented in Figures 14 and 15, and calculated values of log s vs 1/T are given in Figures 16 and 17. Results of the fitted parametric equations are summarized in Table 5. The overall system has been defined for a number of temperatures in Figure 18, and the solubility surface for $PbCl_2$ in 0.1 M $FeCl_3$ is given in Figure 19. Calculated heats of solution are given in Table 6 and the equation parameters used to generate Figure 18 are given in Table 7.

The $PbCl_2$ solubility curves (Table 5a) for 0.1 M $FeCl_3$ - 0.1 to 0.55 M HCl (the common ion effect region) are shown in Figure 12. The spacings between these curves are smaller than those in Figure 4; i.e., the presence of 0.1 M $FeCl_3$ appears to depress the $PbCl_2$ solubility significantly at low total Cl concentrations. The curves for 0.1 M $FeCl_3$ and 1.0 to 3.0 M HCl in Figure 13 (complexation region), however, show a slightly enhanced $PbCl_2$ solubility compared to those in Figure 5. These observations indicate an

increase in free Cl^- concentration due to the 0.1 M $FeCl_3$ that must be dissociated to an appreciable extent in solutions up to 3.0 M HCl.

The density lines (Table 5b, Figures 14 and 15) display a behaviour similar to that noted for the $PbCl_2$ - HCl system, but are shifted to slightly higher values because of the contribution of the 0.1 M $FeCl_3$. The variation of the slopes of these lines is rather erratic, and this may be associated with changes in solution structure due to different types of iron complexes at different HCl concentrations (colour variations) in addition to the $PbCl_2$ contributions.

The logarithmic solubility lines (Table 5c, Figues 16 and 17) also indicate the compression of the data in the common ion effect region caused by the dissociation of $FeCl_3$ (compare Figures 8 and 16). The calculated heats of solution (Table 6) oscillate slightly as a function of the HCl concentration and the two most endothermic ΔH's are found at 0.3 and 1.0 M HCl, whereas the minimum $PbCl_2$ solubility is now located at 1.0 M HCl. Such behaviour might again be related to the formation of different types of ferric chloride complexes at different HCl concentrations and temperatures.

The major effects of adding 0.1 M $FeCl_3$, which appears to contribute free Cl^- ions to the solution, are evident from the solubility isotherms (Table 7) shown in Figure 18. Compared to Figure 10, a shallower drop at low HCl concentrations and a slightly steeper rise at high HCl levels are evident. At first glance, Figure 18 seems to be a good representation of the right-hand side of Figure 10, with a shift corresponding to the maximum Cl^- contribution from the 0.1 M $FeCl_3$ (about 10 g/L). Superposition of the figures in this manner shows, however, that a good fit is obtained only at low HCl concentrations and at low temperatures. This is reasonable since $FeCl_3$ dissociation will be high at low total Cl^- levels, and more complex behaviour can be expected at higher temperatures and Cl concentrations.

The three-dimensional $PbCl_2$ solubility surface shown in Figure 19 also appears as a good representation of the left-hand side of Figure 11, again shifted by about 10 g/L HCl. Thus the surface in Figure 19 appears to be flatter, especially in the low temperature region. The maximum $PbCl_2$ solubility on this surface was 20.5 g/L at 3.0 M HCl and 100°C. The highest points on the $PbCl_2$ solubility surface in the absence of $FeCl_3$ (Figure 11), were 25.4 g/L at 0.1 M HCl and 18.1 g/L at 3.0 M HCl, both at 100°C. Ferrous levels determined by titration following the solubility measurements were less than 0.1 g/L, indicating practically no reduction of the ferric ion.

Table 5 - Solubility and density data as a function of temperature for the aqueous $PbCl_2$ - 0.1 M $FeCl_3$ - HCl system containing 0.1 to 3.0 M HCl.

Conc. HCl (M)	Fitted Equation Parameters A	B	C	Correlation Coefficients
a) Solubility vs Temperature: $S = At \times e^{Bt} + C$				
0.1	0.03980	0.01425	0.5779	0.99832
0.175	0.03509	0.01489	0.5371	0.99935
0.3	0.03109	0.01622	0.2135	0.99741
0.55	0.02198	0.01852	0.4849	0.99909
1.0	0.02513	0.01658	0.2009	0.99885
2.0	0.02961	0.01711	0.2714	0.99843
3.0	0.04370	0.01488	1.1630	0.99946
b) Density vs Temperature: $d = At + B$				
0.1	-0.0002809	1.0202		0.89357
0.175	-0.0003329	1.0248		0.99267
0.3	-0.0003261	1.0260		0.99121
0.55	-0.0003649	1.0310		0.97875
1.0	-0.0003620	1.0387		0.96830
2.0	-0.0003129	1.0541		0.99375
3.0	-0.0003960	1.0813		0.95226
c) Log Solubility vs 1/T: $\text{Log } s = A \times (1000/T) + B$				
0.1	-1.4402	4.1111		0.99378
0.175	-1.4266	4.0334		0.99813
0.3	-1.5953	4.4929		0.99746
0.55	-1.5481	4.3022		0.99840
1.0	-1.5854	4.3782		0.99729
2.0	-1.5832	4.4526		0.99893
3.0	-1.3036	3.7740		0.99893

d = density of saturated solution (g/mL);
S = $PbCl_2$ solubility (g/L); s = $PbCl_2$ solubility (g/100 g solution);
t = temperature (20 to 100°C); T = absolute temperature (K).

Table 6 - Calculated $PbCl_2$ heats of solution in aqueous solutions containing 0.1 M $FeCl_3$ at different HCl concentrations.

HCl (M)	0.1	0.175	0.3	0.55	1.0	2.0	3.0
$\Delta H_{Sol'n}$ (kJ/mol)	27.6	27.4	30.6	29.7	30.5	30.4	25.0

Table 7 - Solubility data as a function of HCl concentration (g/L) for the aqueous $PbCl_2$ - 0.1 M $FeCl_3$ - HCl system at selected temperatures between 20 and 100°C.

Temp.	Fitted Equation Parameters*				
(°C)	A	B	C x 10^4	D x 10^2	E
20	3.89	-0.112	3.421	-2.977	1.492
40	- 9.94	6.813	4.119	-2.788	2.380
50	-11.12	8.397	4.523	-2.799	3.284
60	-30.59	16.56	4.950	-2.277	4.024
70	-39.83	21.12	5.491	-2.096	5.387
80	-51.75	26.57	6.119	-1.857	7.166
90	-63.68	31.81	6.931	-1.722	9.559
100	-75.37	36.65	7.836	-1.615	12.71

*see Equation 8: $S_t = A/c^2 + B/c + Cc^2 + Dc + E$ (g/L).

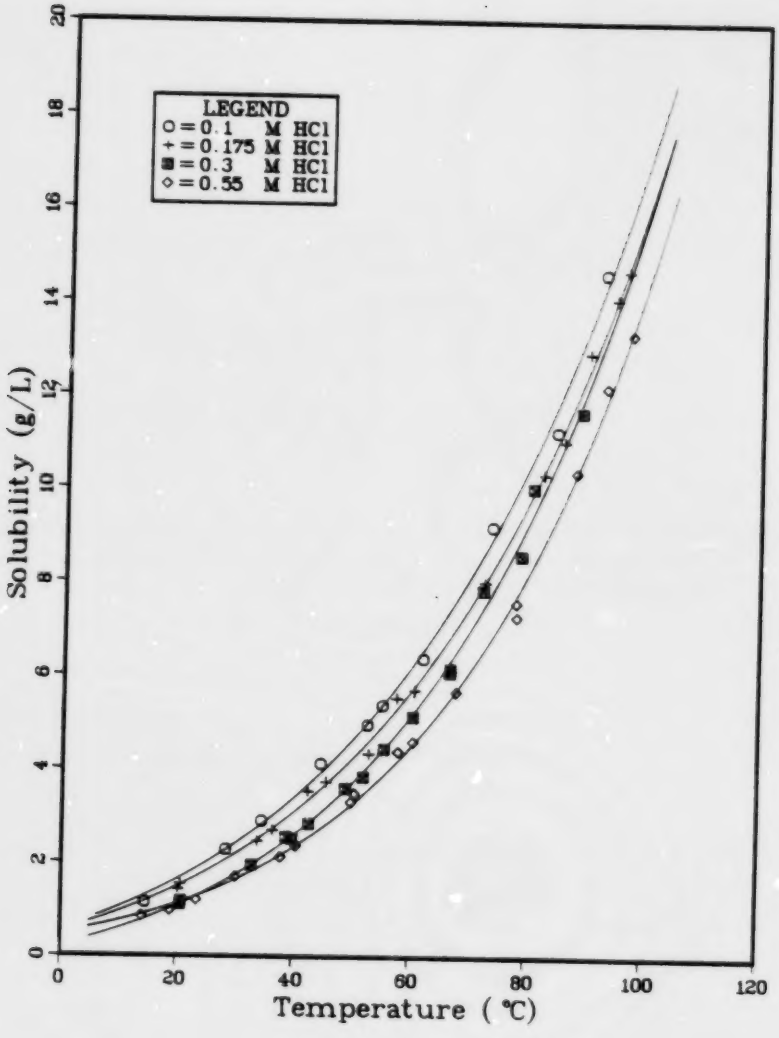

Fig. 12 - Solubility of $PbCl_2$ as a function of temperature for aqueous solutions containing 0.1 M $FeCl_3$ and 0.1 to 0.55 M HCl.

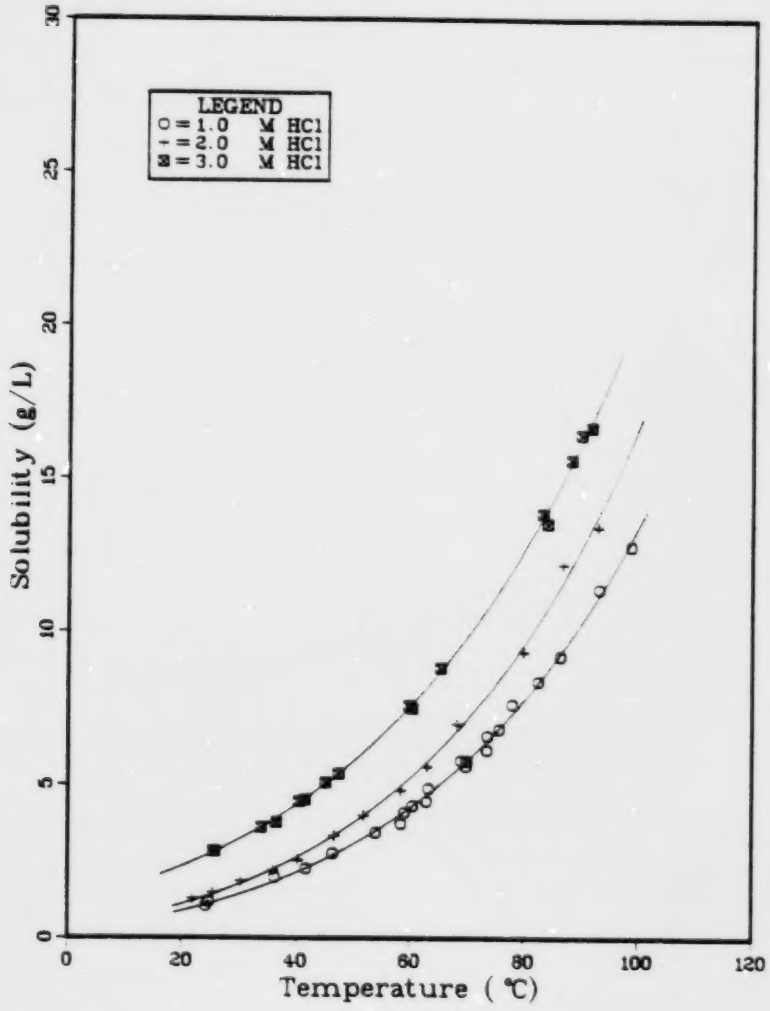

Fig. 13 - Solubility of $PbCl_2$ as a function of temperature for aqueous solutions containing 0.1 M $FeCl_3$ and 1.0 to 3.0 M HCl.

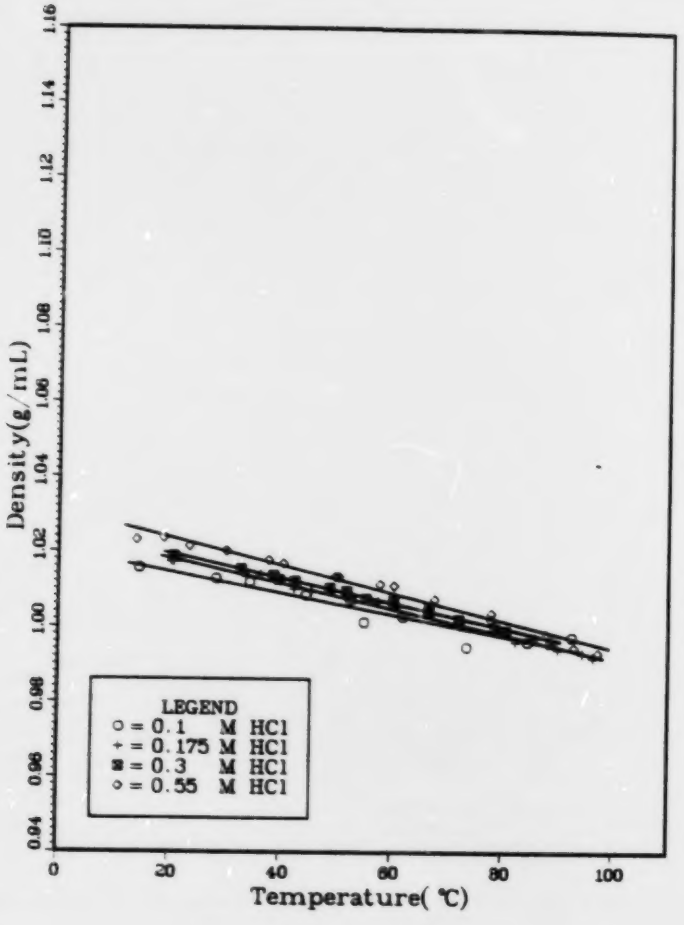

Fig. 14 - Density as a function of temperature for saturated solutions of $PbCl_2$ containing 0.1 M $FeCl_3$ and 0.1 to 0.55 M HCl.

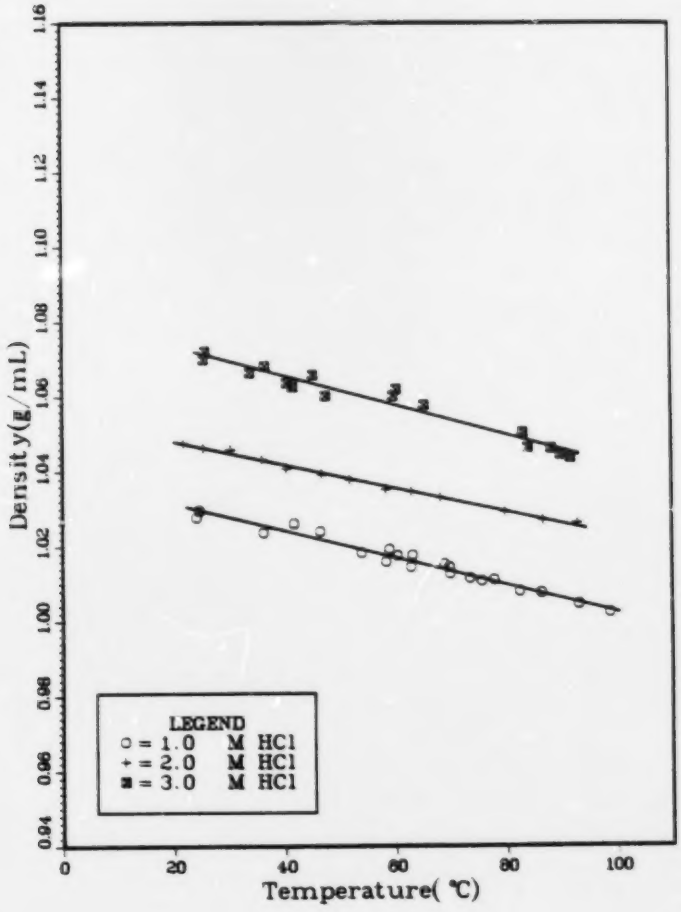

Fig. 15 - Density as a function of temperature for saturated solutions of $PbCl_2$ containing 0.1 M $FeCl_3$ and 1.0 to 3.0 M HCl.

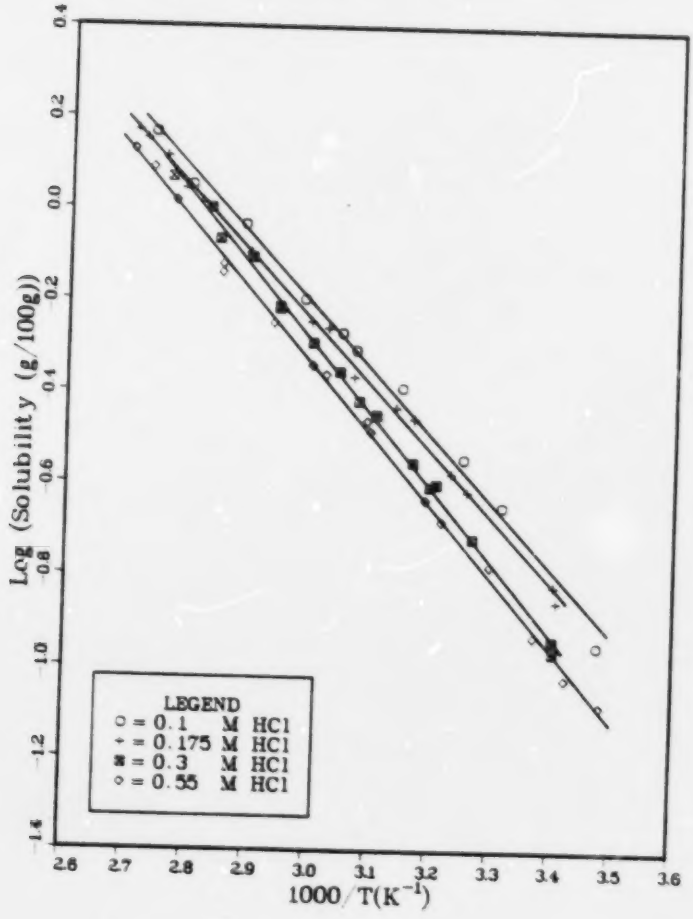

Fig. 16 - The logarithm of the $PbCl_2$ solubility as a function of the reciprocal of the absolute temperature for aqueous solutions containing 0.1 M $FeCl_3$ and 0.1 to 0.55 M HCl.

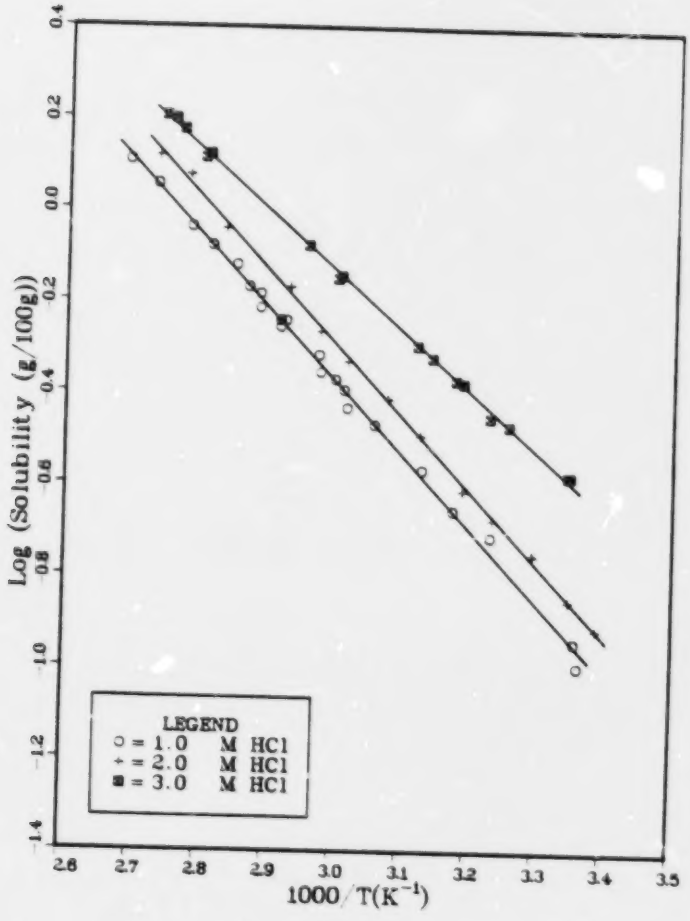

Fig. 17 - The logarithm of the $PbCl_2$ solubility as a function of the reciprocal of the absolute temperature for aqueous solutions containing 0.1 M $FeCl_3$ and 1.0 to 3.0 M HCl.

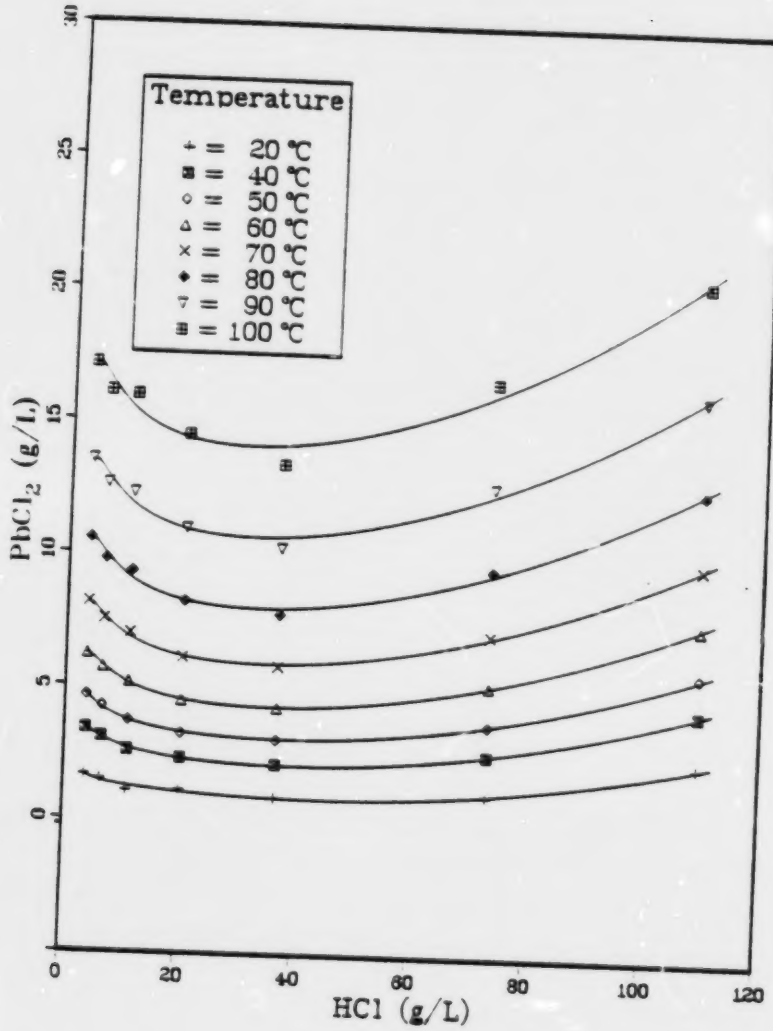

Fig. 18 - Solubility of $PbCl_2$ as a function of HCl concentration in 0.1 M $FeCl_3$, for selected temperatures between 20 and 100°C, as obtained from the 'best fit' parameters given in Table 7.

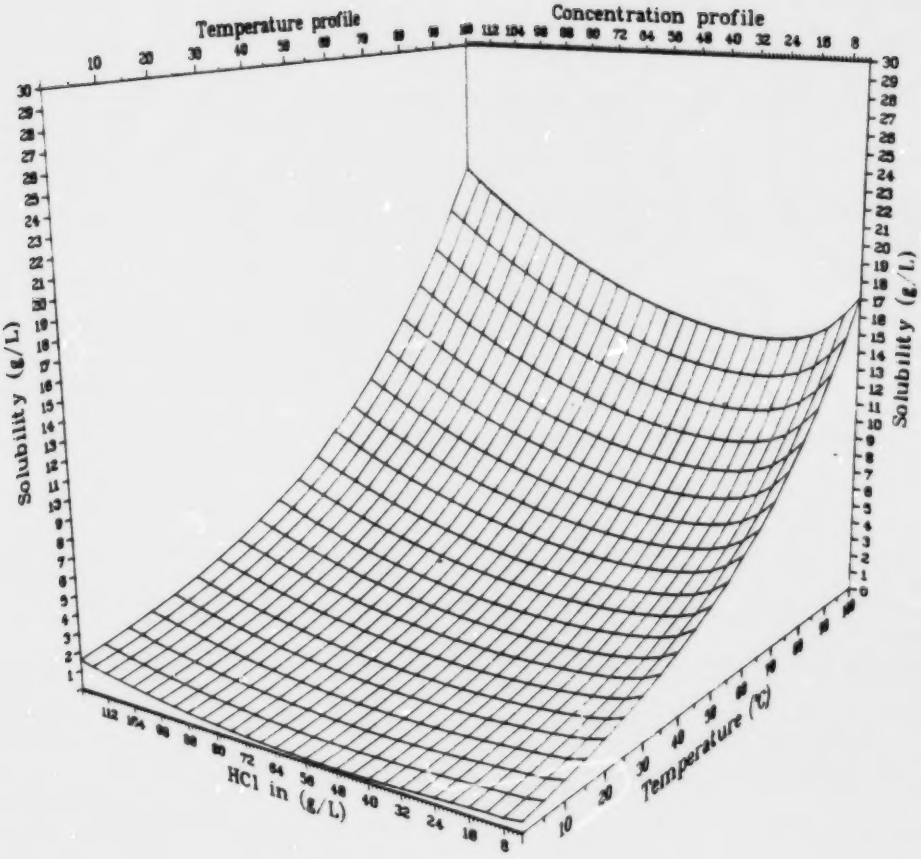

Fig. 19 - The $PbCl_2$ solubility 'surface' in 0.1 M $FeCl_3$ as a function of HCl concentration and temperature.

b) The Aqueous $PbCl_2$ - 0.3 M $FeCl_3$ - HCl System

This section reports $PbCl_2$ solubilities in solutions containing 0.3 M $FeCl_3$ and 0.1, 0.175, 0.3, 0.55, 1.0, 1.5 and 3.0 M HCl. Results of the solubility measurements are given in Figures 20 and 21. The corresponding densities of the saturated $PbCl_2$ solutions are presented in Figures 22 and 23, and calculated values of log s vs 1/T are given in Figures 24 and 25. Results of the fitted parametric equations are summarized in Table 8. The overall system has been defined for a number of temperatures in Figure 26 and the solubility surface for $PbCl_2$ in 0.3 M $FeCl_3$ is given in Figure 27. Calculated heats of solution are presented in Table 9 and the equation parameters used to generate Figure 27 are listed in Table 10.

The trends noted in the preceding sections for the addition of 0.1 M $FeCl_3$ continue for solutions containing 0.3 M $FeCl_3$. The $PbCl_2$ solubility curves (Table 8a) in the common ion effect region (0.1 to 0.55 M HCl) are shown in Figure 20. Compression of the data by free Cl^- ions contributed by the 0.3 M $FeCl_3$ resulted in very little distinction between the curves at 0.1, 0.175, 0.3 and 0.55 M HCl. The behaviour in the complexation region (Figure 21), however, is almost identical to the curves obtained in the presence of only 0.1 M $FeCl_3$ (Figure 13). These observations indicate that 0.3 M $FeCl_3$ is still dissociated to a significant extent at low total Cl^- levels, but that at higher HCl concentrations the contribution of free Cl^- to the solution is about equal to that of the 0.1 M $FeCl_3$ solution. Thus, higher ferric-chloro complex formation appears to occur; e.g., according to:

$$FeCl_3 + Cl^- = FeCl_4^- \qquad (13)$$

The density lines (Table 8b, Figures 22 and 23) display a behaviour in terms of spacing similar to that discussed previously for the 0 and 0.1 M $FeCl_3$ solutions. Variations in the slopes of these curves are even less

regular than in the 0.1 M $FeCl_3$ media because of the diminished relative contributions of $PbCl_2$ and the increased extent of iron complexation. Preliminary calculations indicate also that larger deviations from the linear additivity model for density contributions are obtained in systems containing $FeCl_3$ in the presence of 3.0 M HCl.

The logarithmic solubility lines (Table 8c, Figures 24 and 25) also follow the previously observed trends in going from 0 to 0.1 M $FeCl_3$. The calculated heats of solution show a less oscillatory behaviour with a more pronounced maximum at 0.3 M HCl compared to the results for $FeCl_3$ (Table 6). The most significant changes in the heats of solution of $PbCl_2$ in going from 0 to 0.1 to 0.3 M $FeCl_3$ are observed at low HCl concentrations, becoming increasingly endothermic in that order. This correlates with the observed $PbCl_2$ solubility depression caused by the free Cl^- contributions from $FeCl_3$ in these regions.

The $PbCl_2$ solubility isotherms as a function of HCl concentration in the presence of 0.3 M $FeCl_3$ (Table 10, Figure 26) appear flatter than for the two previous solution systems (0 and 0.1 M $FeCl_3$). Compared to Figure 18 (0.1 M $FeCl_3$), a further shift to higher Cl^- concentrations by about 10 g/L $PbCl_2$ results in an excellent overlap of major portions of the isotherms. Since the difference in $FeCl_3$ concentration of 0.2 M is equivalent to a maximum difference of 0.6 M (21 g/L) free Cl^-, the dissociation of 0.3 M $FeCl_3$ is significantly reduced compared to the 0.1 M $FeCl_3$ solutions, even at low HCl concentrations. By direct comparison (zero HCl shift), the $PbCl_2$ solubility at 3.0 M HCl is similar in solutions containing 0.1 or 0.3 M $FeCl_3$. Hence, iron complexation according to Equation 13 is enhanced by higher $FeCl_3$ concentrations, entirely in accordance with the law of mass action.

The three-dimensional $PbCl_2$ surface of Figure 27 is again much flatter than the one shown in Figure 19 for 0.1 M $FeCl_3$. The above discussion has already established that a shift along the HCl concentration axis by about 10 g/L would again cause a reasonable fit of the two surfaces. The maximum $PbCl_2$ solubility in Figure 27 is 20.6 g/L at 3 M HCl and 100°C, i.e., almost identical to the maximum of Figure 19.

Table 8 - Solubility and density data as a function of temperature for the aqueous $PbCl_2$ - 0.3 M $FeCl_3$ - HCl system containing 0.1 to 3.0 M HCl.

Conc. HCl (M)	Fitted Equation Parameters A	B	C	Correlation Coefficients
a) Solubility vs Temperature: $S = At \times e^{Bt} + C$				
0.1	0.02868	0.01567	0.1837	0.99714
0.175	0.03123	0.01510	0.1618	0.99966
0.3	0.03334	0.01398	3.19E-9	0.99778
0.55	0.02605	0.01640	0.2646	0.99862
1.0	0.01555	0.02200	0.6309	0.99944
1.5	0.02515	0.01823	0.5246	0.99972
3.0	0.04194	0.01540	0.9820	0.99899
b) Density vs Temperature: $d = At + B$				
0.1	-0.0003708	1.0504		0.99069
0.175	-0.0004333	1.0523		0.95911
0.3	-0.0003637	1.0531		0.96422
0.55	-0.0004158	1.0601		0.95077
1.0	-0.0003586	1.0636		0.98449
1.5	-0.0003456	1.0719		0.98933
3.0	-0.0003427	1.1186		0.94978
c) Log Solubility vs 1/T: $\text{Log } s = A \times (1000/T) + B$				
0.1	-1.5489	4.2942		0.99658
0.175	-1.5568	4.3316		0.99878
0.3	-1.5808	4.3865		0.99762
0.55	-1.5342	4.2362		0.99763
1.0	-1.5217	4.1796		0.99287
1.5	-1.5101	4.2188		0.99833
3.0	-1.3453	3.8664		0.99635

d = density of saturated solution (g/mL);
S = $PbCl_2$ solubility (g/L); s = $PbCl_2$ solubility (g/100 g solution);
t = temperature (20 to 100°C); T = absolute temperature (K).

Table 9 - Calculated $PbCl_2$ heats of solution in aqueous solutions containing 0.3 M $FeCl_3$ at different HCl concentrations.

HCl (M)	0.1	0.175	0.3	0.55	1.0	1.5	3.0
$\Delta H_{Sol'n}$ (kJ/mol)	29.7	29.9	30.3	29.4	29.2	29.0	25.8

Table 10 - Solubility data as a function of HCl concentration (g/L) for the aqueous $PbCl_2$ - 0.3 M $FeCl_3$ - HCl system at selected temperatures between 20 and 100°C.

Temp. (°C)	Fitted Equation Parameters* A	B	C x 10^4	D x 10^2	E
20	- 5.29	2.673	0.453	0.864	0.609
40	-10.83	7.552	1.584	0.364	1.735
50	-28.86	10.84	2.039	0.445	2.499
60	-39.05	14.78	2.304	0.929	3.432
70	-50.24	19.46	2.242	2.016	4.563
80	-62.15	24.90	1.668	3.973	5.929
90	-74.28	31.14	0.326	7.160	7.573
100	-85.86	38.16	-2.128	12.05	9.543

*see Equation 8: $S_t = A/c^2 + B/c + Cc^2 + Dc + E$ (g/L).

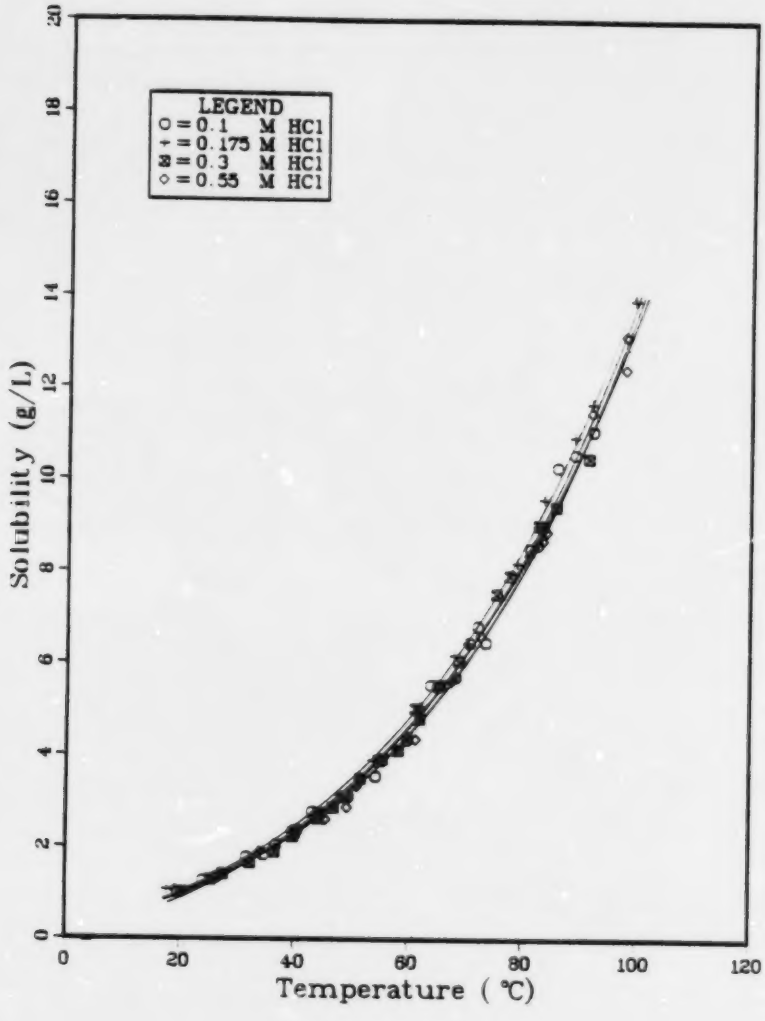

Fig. 20 - Solubility of $PbCl_2$ as a function of temperature for aqueous solutions containing 0.3 M $FeCl_3$ and 0.1 to 0.55 M HCl.

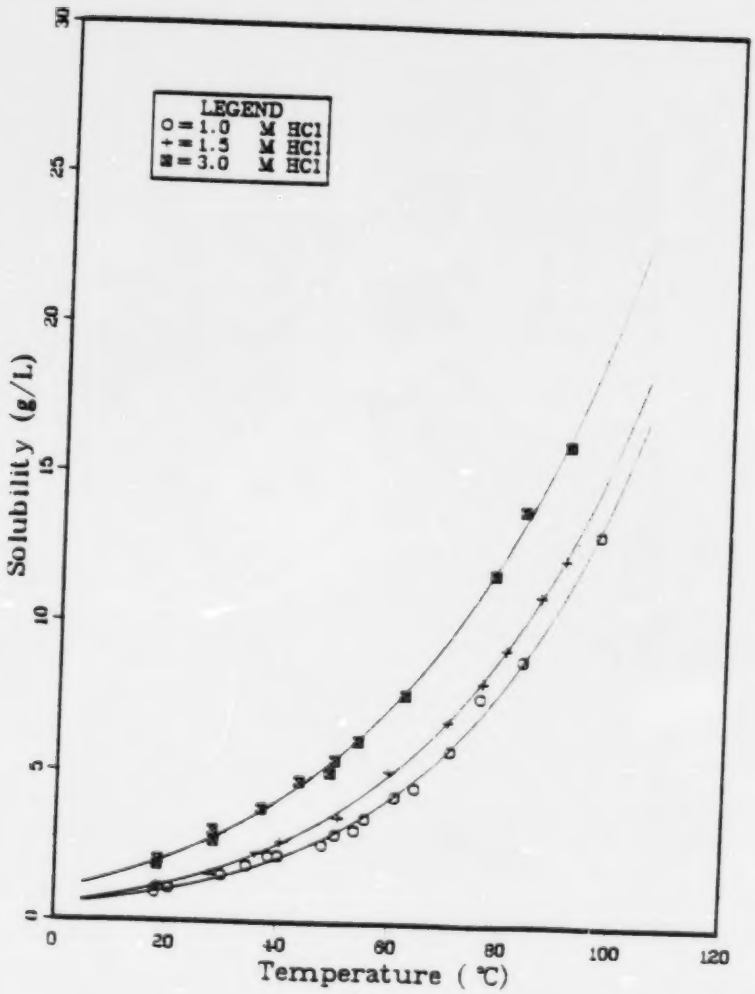

Fig. 21 - Solubility of $PbCl_2$ as a function of temperature for aqueous solutions containing 0.3 M $FeCl_3$ and 1.0 to 3.0 M HCl.

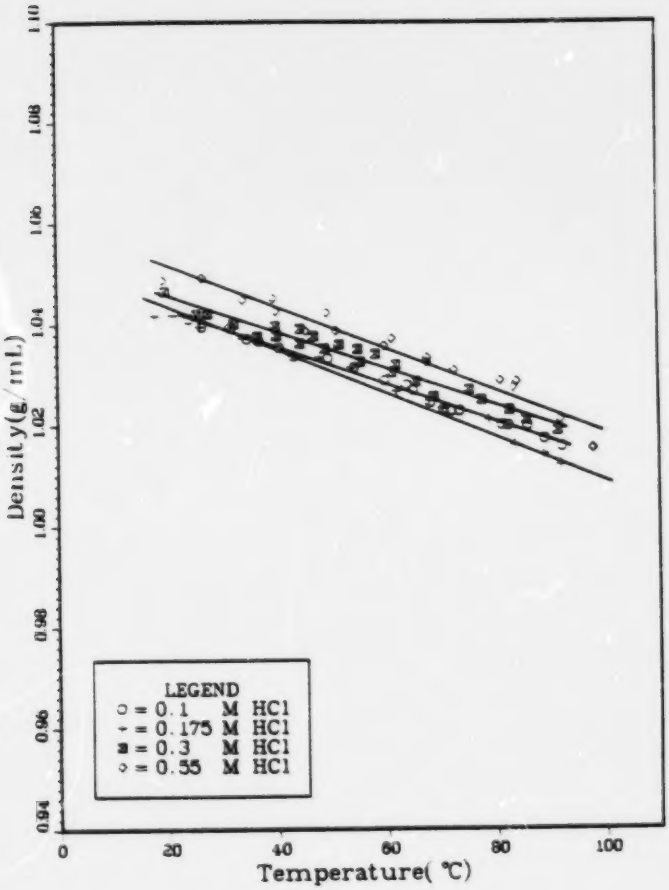

Fig. 22 - Density as a function of temperature for saturated solutions of $PbCl_2$ containing 0.3 M $FeCl_3$ and 0.1 to 0.55 M HCl.

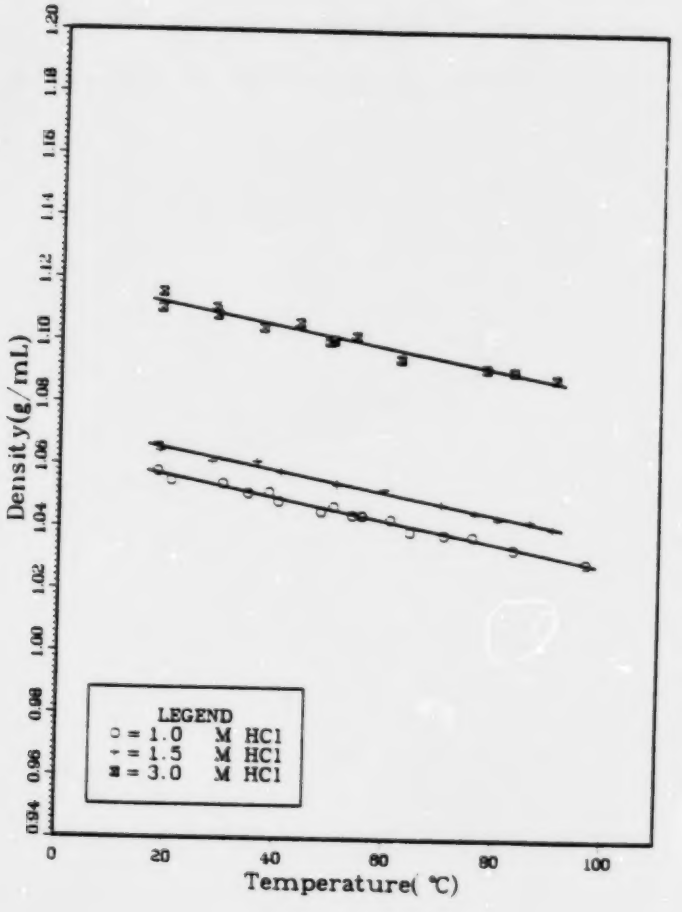

Fig. 23 - Density as a function of temperature for saturated solutions of $PbCl_2$ containing 0.3 M $FeCl_3$ and 1.0 to 3.0 M HCl.

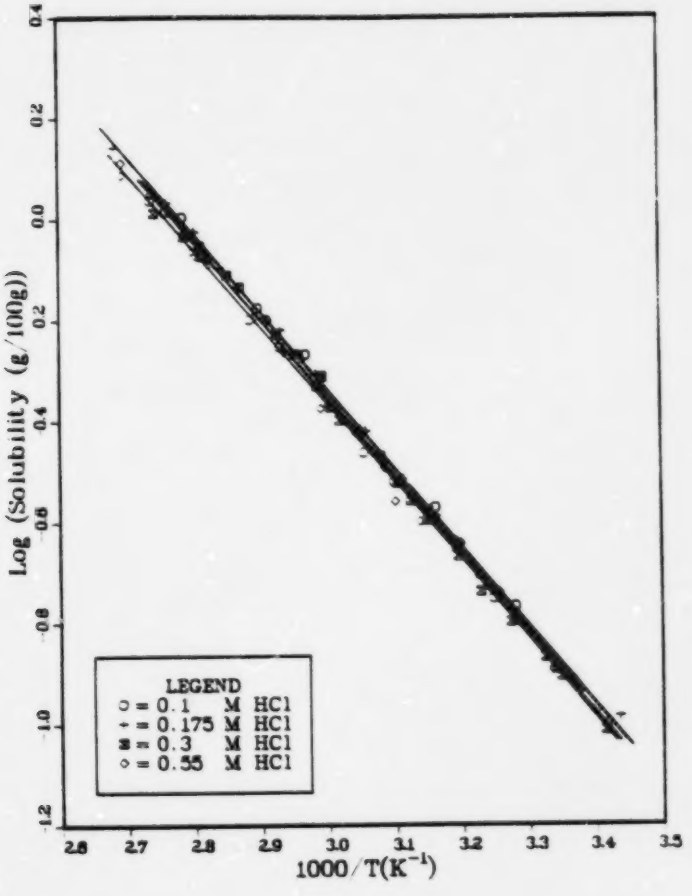

Fig. 24 - The logarithm of the $PbCl_2$ solubility as a function of the reciprocal of the absolute temperature for aqueous solutions containing 0.3 M $FeCl_3$ and 0.1 to 0.55 M HCl.

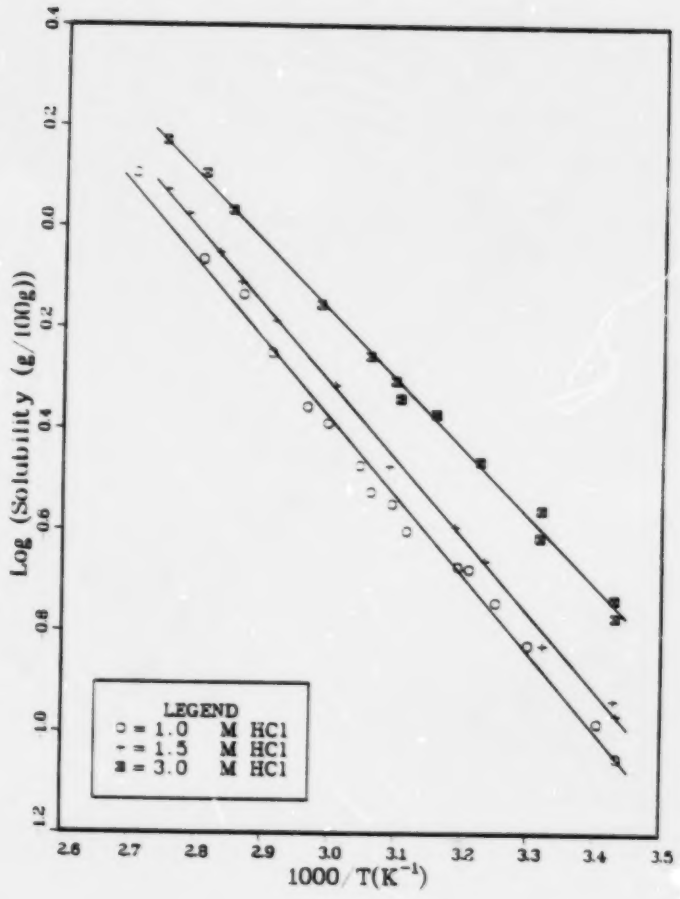

Fig. 25 - The logarithm of the $PbCl_2$ solubility as a function of the reciprocal of the absolute temperature for aqueous solutions containing 0.3 M $FeCl_3$ and 1.0 to 3.0 M HCl.

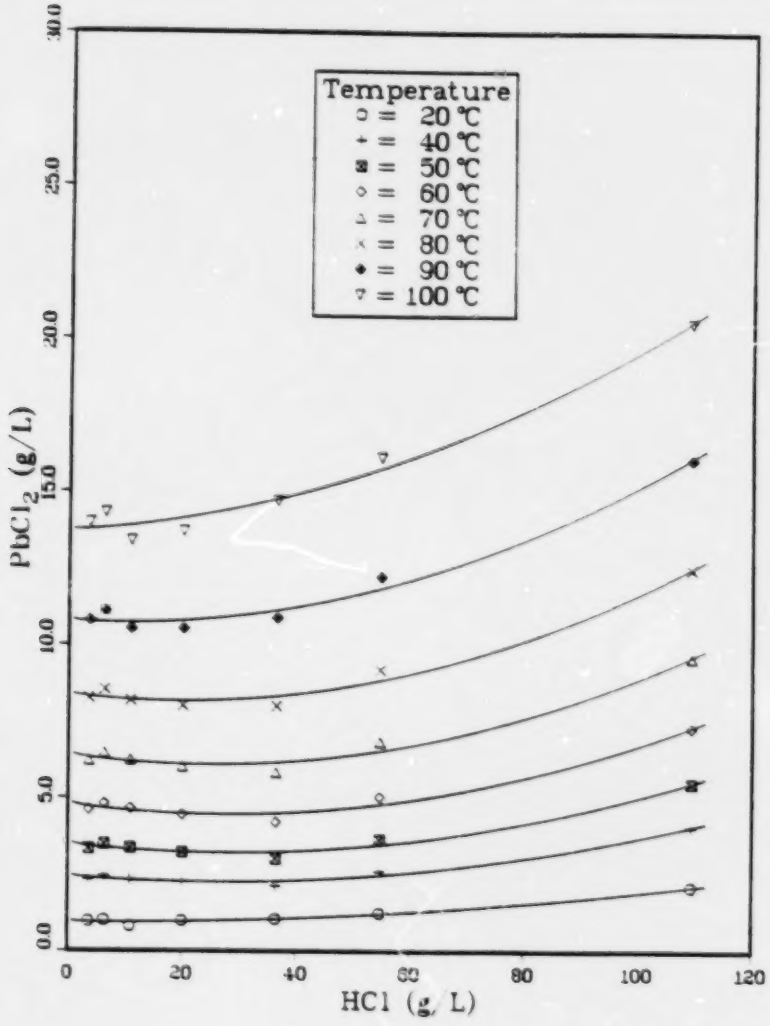

Fig. 26 - Solubility of $PbCl_2$ as a function of HCl concentration in 0.3 M $FeCl_3$, for selected temperatures between 20 and 100°C, as obtained from the 'best fit' parameters given in Table 10.

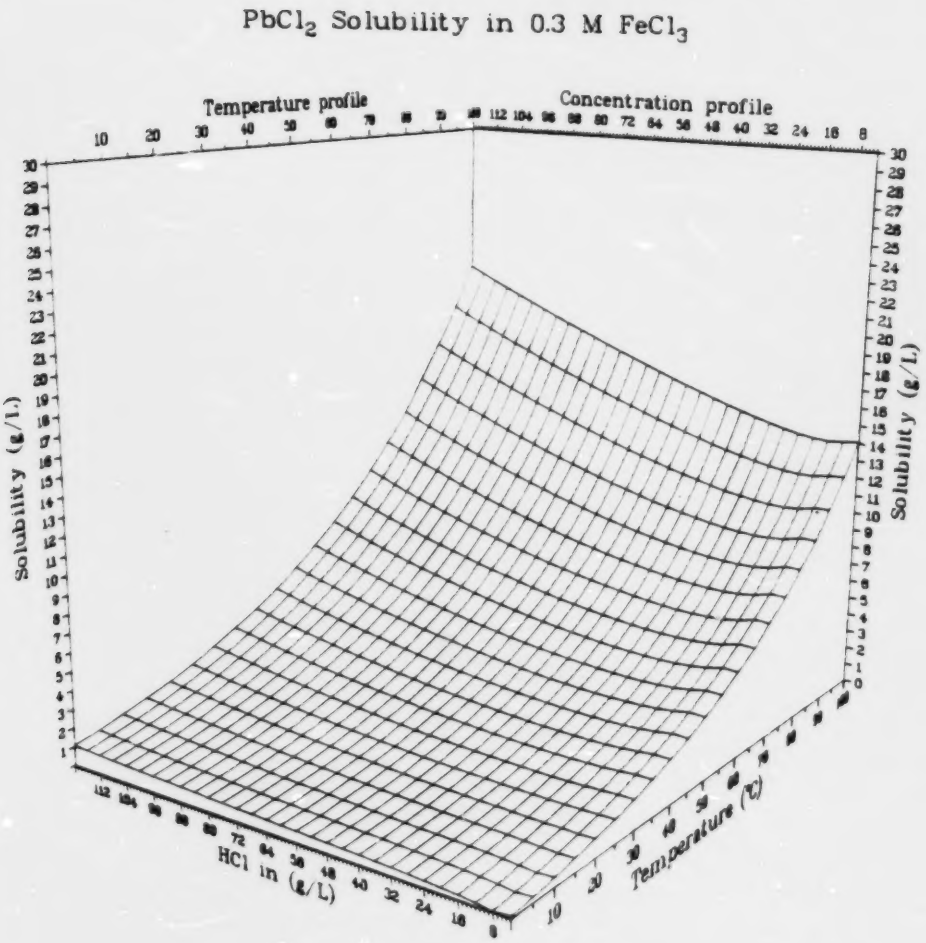

Fig. 27 - The $PbCl_2$ solubility 'surface' in 0.3 M $FeCl_3$ as a function of HCl concentration and temperature.

c) The Aqueous $PbCl_2$ - 1.0 M HCl - $FeCl_3$ System

This section reports $PbCl_2$ solubilities in aqueous solutions of 1.0 M HCl containing 0.3, 0.55, 1.0, 2.0 and 3.0 M $FeCl_3$. Thus, the measured solubilities are reported as a function of varying ferric ion concentration whereas the previous results reported $PbCl_2$ solubilities at a constant $FeCl_3$ concentration but at various concentrations of HCl. Results of the solubility and density measurements are given in Figures 28 and 29, respectively. Calculated values of log s vs 1/T are shown in Figure 30. Results of the fitted parametric equations are summarized in Table 11. The overall system has been defined for a number of temperatures in Figure 31, and the solubility surface for $PbCl_2$ in 1.0 M HCl and 0.3 to 3.0 M $FeCl_3$ is given in Figure 32. Calculated heats of solution are given in Table 12 and the equation parameters used to generate Figure 32 are presented in Table 13.

The $PbCl_2$ solubility curves (Table 11a, Figure 28) display the expected behavour below 70°C, increasing steadily with higher $FeCl_3$ concentrations in the complexation region above 0.3 M $FeCl_3$. The curves in the "common ion effect" region (0, 0.1, 0.3 M $FeCl_3$) overlap extensively and only the 0.3 M $FeCl_3$ curve is shown; data for the lower concentrations can be found in the previous sections. At higher temperatures, however, large $FeCl_3$ additions depress the $PbCl_2$ solubility. Thus, the 3.0 M $FeCl_3$ curve cuts across all other curves, indicating that a substantial withdrawal of free Cl^- occurs.

Possible explanations of this behaviour include Fe^{3+} complexation according to Equation 13 of the preceding section, or the formation of polynuclear Fe^{3+} complexes, or the drastic activity coefficient changes generally associated with concentrated brines (10-13,21-23). The overall trends were established by repeated measurements and the constancy of the ferric concentration in solution was also ascertained. The "ionic saturation effect" at high $FeCl_3$ levels appears to occur at the expense of the $PbCl_2$

only, and recent ferric chloride leaching experiments on galena (24) confirm these observations.

The density lines (Table 11b, Figure 29) are much more widely spaced than those at constant $FeCl_3$ and varying HCl concentrations (see previous sections). This and the fact that the lines below 3.0 M $FeCl_3$ are relatively parallel may be attributed to the much more significant contribution of $FeCl_3$ to the overall solution density, compared to either HCl or $PbCl_2$. The much steeper negative slope of the 3.0 M $FeCl_3$ line, however, correlates with the depression of the $PbCl_2$ solubility, especially in the high temperature region. Since the linear additivity rule for contributions by various solutes appears to break down for concentrated solutions, other effects related to the solution structure should also be taken into consideration.

The logarithmic solubility lines (Table 11c, Figure 30) differ from those of the systems with constant $FeCl_3$ concentration. The tendency for crossover in relatively low temperature regions is evident from the slopes and the monotonically decreasing heats of solution calculated from these slopes (Table 12). It should be noted that the 1.0 M HCl concentration of these solutions already corresponds to the transition region of the previously discussed constant $FeCl_3$ concentration systems. Consequently, the common ion effect is practically non-existent in this particular case.

The $PbCl_2$ solubility isotherms as a function of $FeCl_3$ concentration (Table 13, Figure 31), therefore, do not display the minimum associated with the common ion effect. Since the plot starts at 1.0 M HCl and 0.3 M $FeCl_3$, Figure 31 actually represents a continuation of Figure 26 (0.3 M $FeCl_3$) around 36.5 g/L HCl. The postulated ionic saturation effect is evident in the convexity of the curves above 70°C.

The three-dimensional $PbCl_2$ solubility surface (Figure 32) is similarly an extension of the surface shown in Figure 27 for 0.3 M $FeCl_3$ solutions with the concentration axis rescaled and shifted by about 36.5g/L HCl. No minimum corresponding to the common ion effect is observed and the total ionic saturation effect renders the surface convex at higher temperatures. The highest $PbCl_2$ solubilities are observed at 100°C between 1.0 and 2.0 M $FeCl_3$ (about 17 g/L); at higher $FeCl_3$ concentrations the $PbCl_2$ solubility drops significantly; i.e., to 14 g/L at 3.0 M and to 12 g/L at 3.5 M $FeCl_3$.

Additional data points were measured to verify the anomalous solubility trend at high $FeCl_3$ concentrations. The results indicate that smaller steps in $FeCl_3$ concentrations may alter the shape of the isotherms slightly, while the observed trends are basically correct. This indicates that much more work is required to establish the detailed $PbCl_2$ solubility behaviour in these highly concentrated solutions, and a discussion of the results will be deferred to a follow-up study.

Table 11 - Solubility and density data as a function of temperature for the aqueous $PbCl_2$ - 1.0 M HCl - $FeCl_3$ system containing 0.3 to 3.0 M $FeCl_3$.

Conc. $FeCl_3$ (M)	Fitted Equation Parameters A	B	C	Correlation Coefficients
a) Solubility vs Temperature: $S = At \times e^{Bt} + C$				
0.3	0.01555	0.02200	0.6309	0.99927
0.55	0.02695	0.01686	0.5485	0.99908
1.0	0.02561	0.01856	0.9730	0.99944
2.0	0.03914	0.01350	1.7321	0.99754
3.0	0.06453	0.00651	2.2714	0.98996
b) Density vs Temperature: $d = At + B$				
0.3	-0.0003586	1.0636		0.98449
0.55	-0.0004109	1.1048		0.82793
1.0	-0.0003531	1.1526		0.93169
2 0	-0.0005620	1.2896		0.87382
3.0	-0.0007719	1.4021		0.88557
c) Log Solubility vs 1/T: $\text{Log } s = A \times (1000/T) + B$				
0.3	-1.5217	4.1796		0.99287
0.55	-1.4724	4.0873		0.99872
1.0	-1.3480	3.7538		0.99740
2.0	-1.1179	3.1159		0.99406
3.0	-0.8220	2.2391		0.99453

d = density of saturated solution (g/mL);
S = $PbCl_2$ solubility (g/L); s = $PbCl_2$ solubility (g/100 g solution);
t = temperature (20 to 100 ^{o}C); T = absolute temperature (K).

Table 12 - Calculated $PbCl_2$ heats of solution in aqueous solutions containing 1.0 M HCl and different $FeCl_3$ concentrations.

$FeCl_3$ (M)	0.0	0.1	0.3	0.55	1.0	2.0	3.0
$\Delta H_{Sol'n}$ (kJ/mol)	30.6	30.5	29.2	28.3	25.9	21.4	15.7

Table 13 - Solubility data as a function of $FeCl_3$ concentration (g/L) for the aqueous $PbCl_2$ - 1.0 M HCL - $FeCl_3$ system at selected temperatures between 20 and 100°C.

Temp.	Fitted Equation Parameters*				
(°C)	A	B	C x 10^6	D x 10^3	E
20	0.058	1.598	1.120	5.411	0.849
30	2.165	- 31.815	8.605	1.510	2.099
40	0.821	- 38.300	5.692	3.192	2.820
50	1.440	- 60.428	6.039	2.707	4.143
60	3.610	- 84.452	4.451	2.838	5.758
70	4.435	-106.04	0.272	3.795	7.726
80	-1.317	-117.63	- 7.342	5.863	10.114
90	2.383	-131.82	-19.942	9.696	12.971
100	-1.258	-125.36	-37.533	15.003	16.451

*see Equation 8: $S_t = A/c^2 + B/c + Cc^2 + Dc + E$ (g/L).

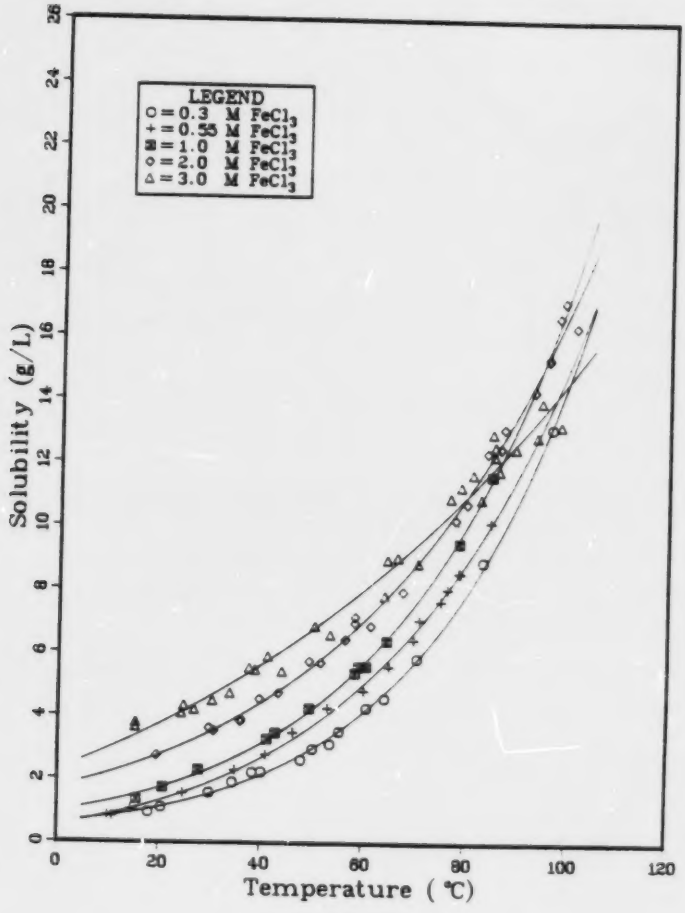

Fig. 28 - Solubility of $PbCl_2$ as a function of temperature for aqueous solutions containing 1.0 M HCl and 0.3 to 3.0 M $FeCl_3$.

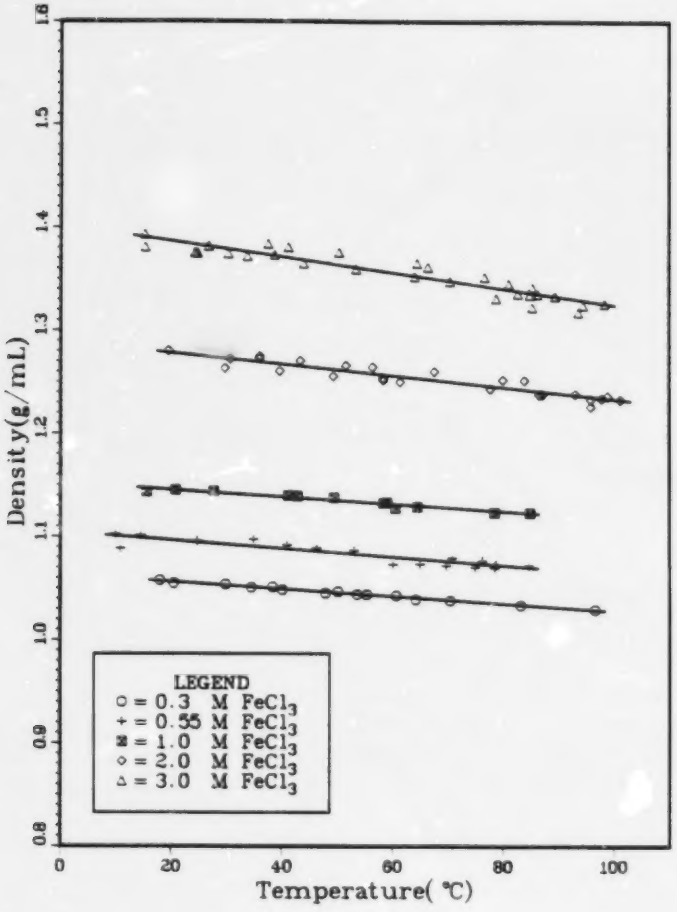

Fig. 29 - Density as a function of temperature for saturated solutions of $PbCl_2$ containing 1.0 M HCl and 0.3 to 3.0 M $FeCl_3$.

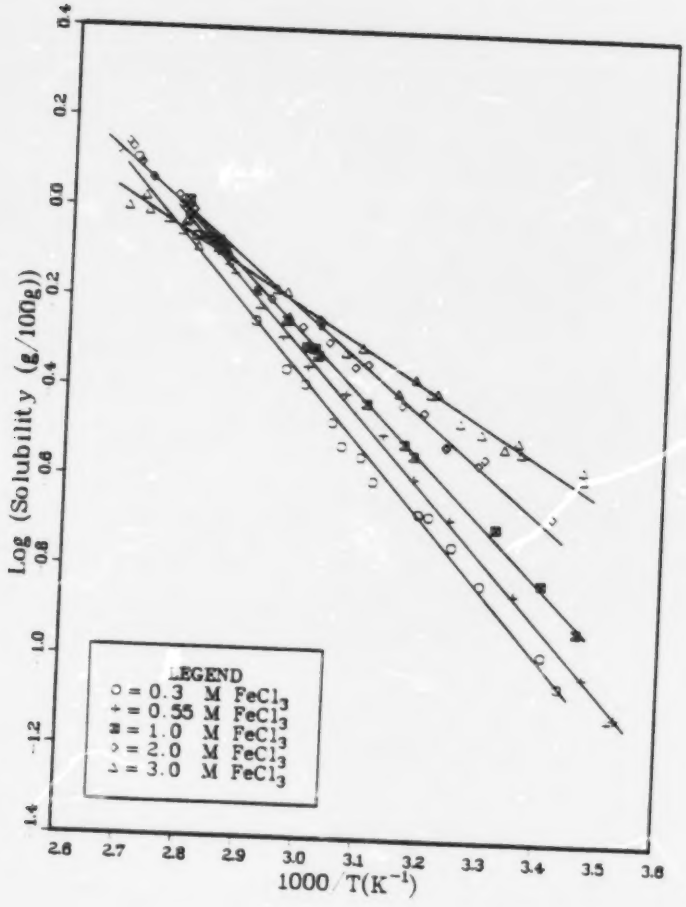

Fig. 30 - The logarithm of the $PbCl_2$ solubility as a function of the reciprocal of the absolute temperature for aqueous solutions containing 1.0 M HCl and 0.3 to 3.0 M $FeCl_3$.

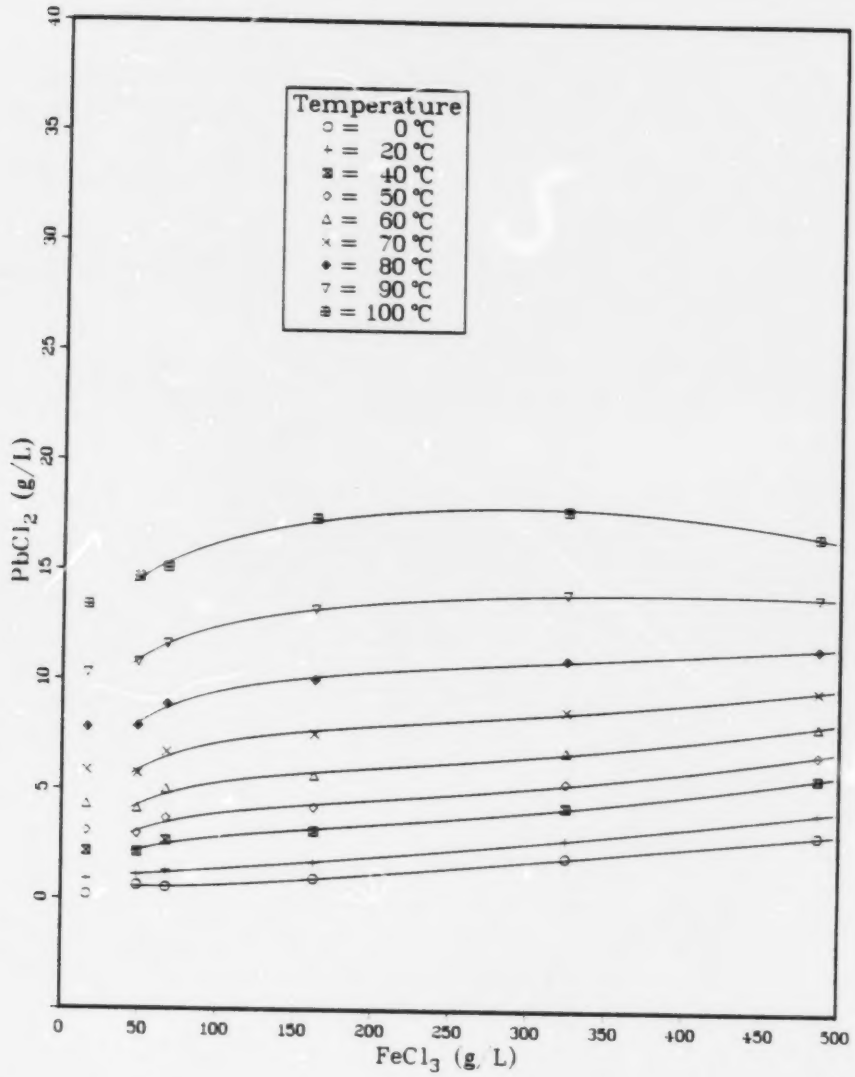

Fig. 31 - Solubility of $PbCl_2$ as a function of $FeCl_3$ concentration in 1.0 M HCl, for selected temperatures between 20 and 100°C, as obtained from the 'best fit' parameters given in Table 13.

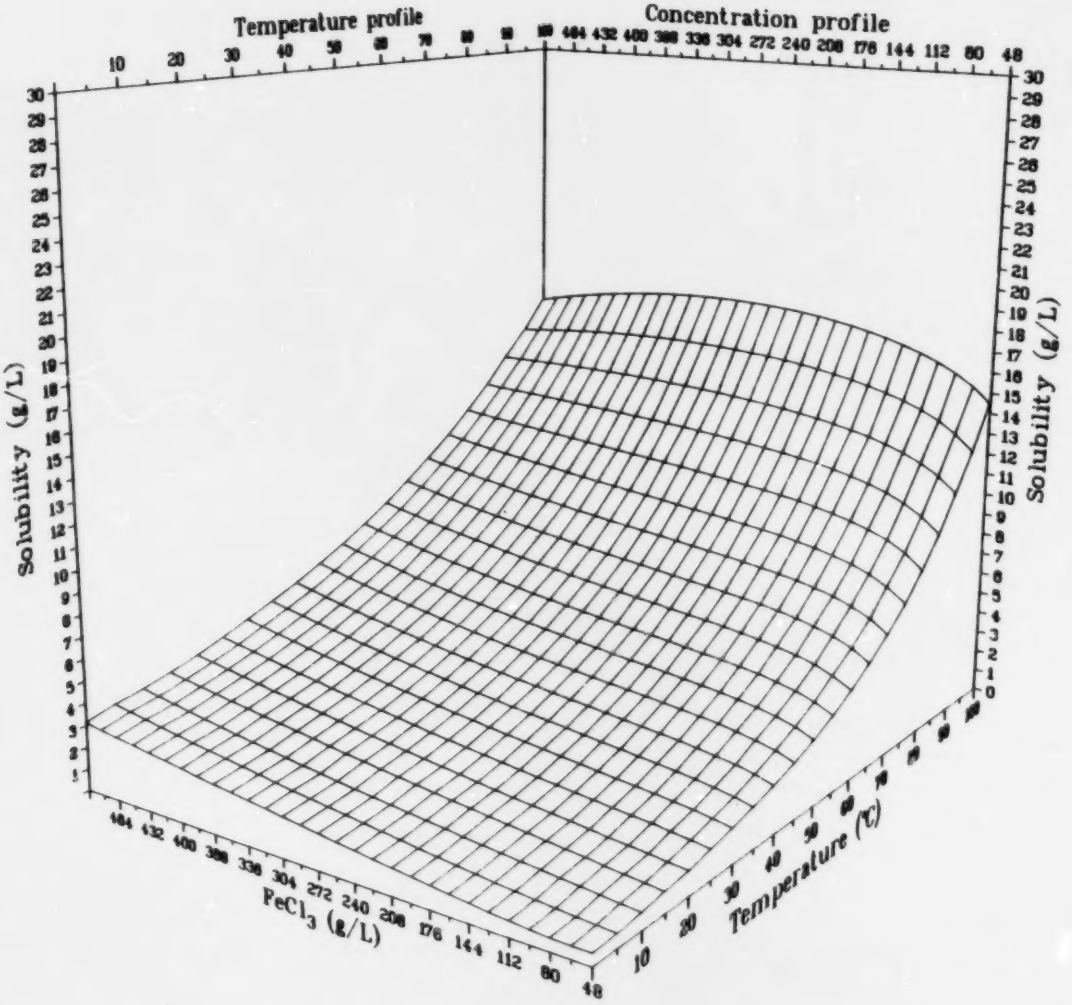

Fig. 32 - The $PbCl_2$ solubility 'surface' in 1.0 M HCl as a function of $FeCl_3$ concentration and temperature.

d) The Aqueous $PbCl_2$ - 1.0 M HCl - 1.0 M $FeCl_3$ - $FeCl_2$ System

This section reports $PbCl_2$ solubilities in aqueous solutions of 1.0 M HCl and 1.0 M $FeCl_3$ containing 0.0, 0.5, 1.0 and 1.5 M $FeCl_2$. The results of the solubility and density measurements are given in Figures 33 and 34, respectively. Calculated values of log s vs. 1/T are presented in Figure 35. Results of the fitted parametric solubility equations in Figure 33 are summarized in Table 14, and the calculated heats of solution are given in Table 15.

The $PbCl_2$ solubility curves as a function of temperature are given in Table 14a and Figure 33. Since 1.0 M HCl and 1.0 M $FeCl_3$ are present in all solutions, these systems are expected to fall in the complexation region only. The 0.0, 0.5 and 1.0 M $FeCl_2$ curves appear to behave in an acceptable manner; i.e., they show parallel increases in solubility corresponding to the increases in free Cl^- concentration. The 1.5 M $FeCl_2$ curve, however, starts off with an even more exaggerated deviation than is observed for 3.0 M $FeCl_3$ in the absence of $FeCl_2$ (Figure 28). It appears that the ionic saturation level is approached at a lower temperature (ca. 60°C), but above 70°C the $PbCl_2$ solubility recovers and is further enhanced compared to the lower $FeCl_2$ concentrations. Since the Fe^{2+}/Fe^{3+} ratios and the total iron concentrations remained constant over the entire temperature range, the observations may be rationalized as follows.

At low temperatures the free Cl^- contributions from $FeCl_2$ may induce the formation of higher chloro-ferrate complexes and other species postulated in the previous section. This results in a net reduction of free Cl^- available for the complexation of $PbCl_2$. Since a limited amount of $FeCl_3$ is available, a point is reached beyond which no further free Cl^- withdrawal is possible and the temperature-induced release of free Cl^- ions by $FeCl_2$ then results in an increase in $PbCl_2$ solubility. The ionic saturation effect may thus

influence ferric and lead species only, or else the corresponding effect on ferric chloride species may be reversed with increasing temperatures.

The density curves shown in Table 14b and Figure 34 behave in a similar manner as those in the $PbCl_2$ - 1.0 M HCl - $FeCl_3$ system (Figure 29) although the decrease in slope at 1.5 M $FeCl_2$ is less appreciable due to the recovery of higher $PbCl_2$ solubilities at the higher temperatures. The logarithmic $FeCl_2$ solubility lines (Table 14c, Figure 35), also display crossover tendencies at some higher temperatures, although the solubility data may better be approximated by the dashed curves. The linear equations were used to calculate average heats of solution (Table 15), which also become monotonically more endothermic.

No isotherms were calculated since Equation 8 no longer fits the measured data. Additional measurements are underway to confirm the anomaly near 1.5 M $FeCl_2$, and a detailed discussion of the results will have to await the completion of this follow-up study. Meanwhile, examination of Figure 33 shows that the $PbCl_2$ solubility tends to increase with increasing $FeCl_2$ concentrations below the 1.5 M level. The three-dimensional $PbCl_2$ solubility surface would therefore appear to be similar to the one shown in Figure 27 for the aqueous $PbCl_2$ - 0.3 M $FeCl_3$ - HCl system. The $PbCl_2$ solubility maximum on this surface will be located at 100°C, 1.5 M $FeCl_2$ (32 g/L), and this to be compared with the already substantial 17.4 g/L $PbCl_2$ solubility at 100°C, in 1 M HCl - 1 M $FeCl_3$ - 0 M $FeCl_2$ solution. In practice, the reduction of the $FeCl_3$ leaching solution by sulphide minerals is expected to increase the $PbCl_2$ solubility drastically. Although not contemplated in the current flowsheet, reoxidation of the $FeCl_2$ solution prior to the $PbCl_2$ crystallization would increase the recovery of $PbCl_2$ during cooling.

Table 14 - Solubility and density data as a function of temperature for the aqueous $PbCl_2$ - 1.0 M HCl - 1.0 M $FeCl_3$ - $FeCl_2$ system containing 0.5 to 1.5 M $FeCl_2$.

Conc. $FeCl_2$ (M)	Fitted Equation Parameters A	B	C	Correlation Coefficients
a) Solubility vs Temperature: $S = At \times e^{Bt} + C$				
0.5	0.03082	0.01857	1.8714	0.99730
1.0	0.03881	0.01742	3.3175	0.99884
1.5	0.00891	0.03335	7.0010	0.99784
b) Density vs Temperature: $d = At + B$				
0.5	-0.0003473	1.2015		0.98725
1.0	-0.0004115	1.2564		0.89636
1.5	-0.0003473	1.2015		0.98725
c) Log Solubility vs 1/T: $\text{Log } s = A \times (1000/T) + B$				
0.5	-1.2405	3.5437		0.98674
1.0	-1.0995	3.2380		0.98890
1.5	-0.8727	2.6465		0.91097

d = density of saturated solution;
S = $PbCl_2$ solubility (g/L); s = $PbCl_2$ solubility (g/100 g solution);
t = temperature (20 to 100°C); T = absolute temperature (K).

Table 15 - Calculated $PbCl_2$ heats of solution in aqueous solutions containing 1.0 M HCl, 1.0 M $FeCl_3$ and different $FeCl_2$ concentrations.

$FeCl_2$ (M)	0.0	0.5	1.0	1.5
$\Delta H_{Sol'n}$ (kJ/mol)	25.9	23.8	21.1	16.7

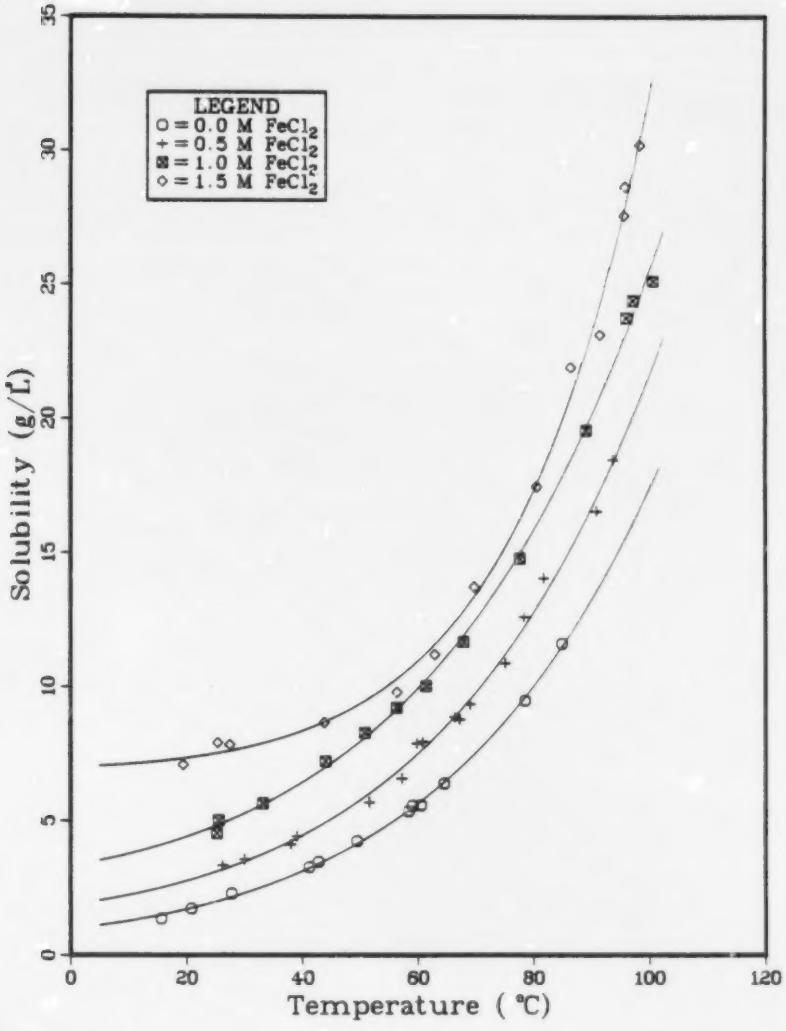

Fig. 33 - Solubility of $PbCl_2$ as a function of temperature for aqueous solutions containing 1.0 M HCl, 1.0 M $FeCl_3$ and 0.0 to 1.5 M $FeCl_2$.

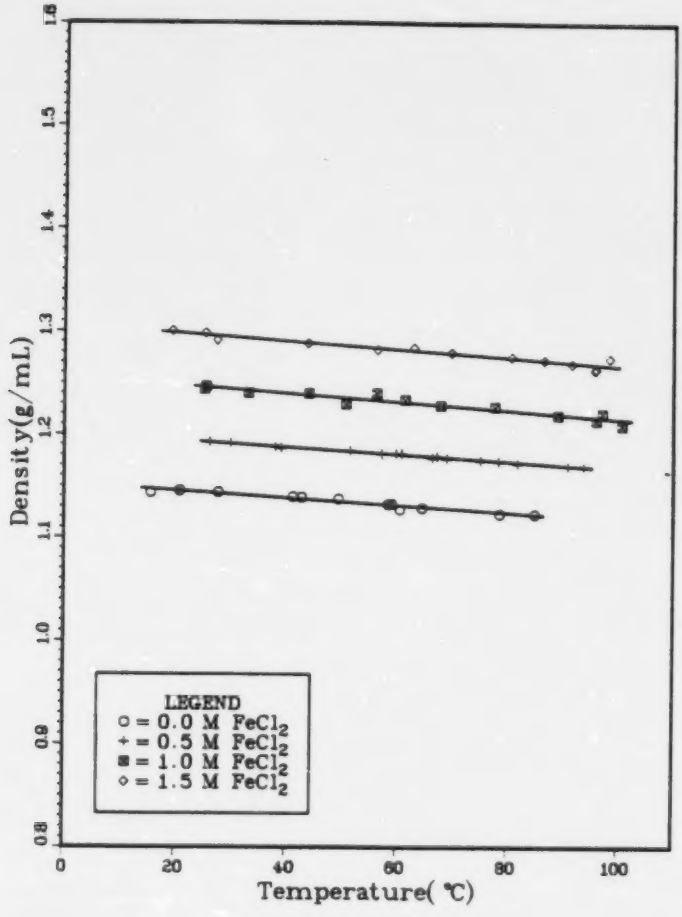

Fig. 34 - Density as a function of temperature for saturated solutions of $PbCl_2$ containing 1.0 M HCl, 1.0 M $FeCl_3$ and 0.0 to 1.5 M $FeCl_2$.

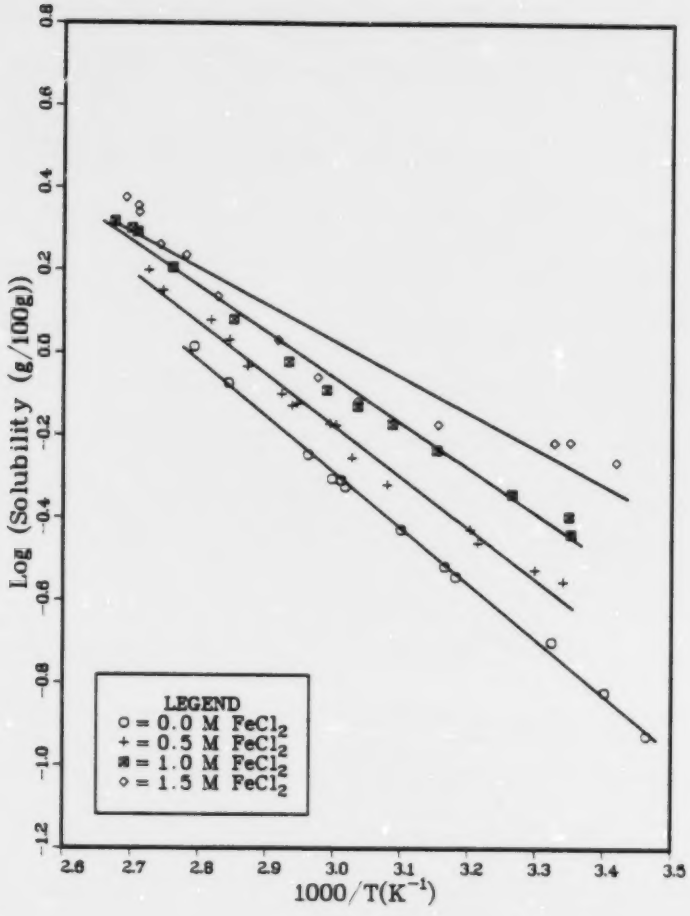

Fig. 35 - The logarithm of the $PbCl_2$ solubility as a function of the reciprocal of the absolute temperature for aqueous solutions containing 1.0 M HCl, 1.0 M $FeCl_3$ and 0.0 to 1.5 M $FeCl_2$.

Lead Chloride Solubilities in the Presence of NaCl and $MgCl_2$

It is well known that the presence of readily dissociable salts of Group IA or IIA cations yields high $PbCl_2$ solubilities by providing free Cl^- to form lead-chloro complexes. Therefore, $PbCl_2$ solubilities and solution densities have been measured in several NaCl and $MgCl_2$ systems in which the salt concentrations were varied over an appreciable range.

a) The Aqueous $PbCl_2$ - 1.0 M HCl - 0.1 M $FeCl_3$ - $MgCl_2$ System

This section reports $PbCl_2$ solubilities in aqueous solutions of 1.0 M HCl and 0.1 M $FeCl_3$ containing 0.0, 0.5, 1.0, 1.5 and 2.2 M $MgCl_2$. Thus, the measured solubilities are reported as a function of chloride concentration (as $MgCl_2$). Results of the solubility and density measurements are given in Figures 36 and 37, respectively. Calculated values of log s vs 1/T are presented in Figure 38. Results of the fitted parametric solubility equations in Figure 36 are summarized in Table 16. Calculated heats of solution are given in Table 17.

The $PbCl_2$ solubility curves as a function of temperature (Table 16a, Figure 36) display a well-behaved monotonic increase with temperature and with $MgCl_2$ concentration. Since the presence of 1 M HCl and 0.1 M $FeCl_3$ in all the solutions corresponds to the transition region between the common ion effect and complexation, all further chloride additions are expected to increase the $PbCl_2$ solubility. The curve for 2.2 M $MgCl_2$ shows the steepest increase in the $PbCl_2$ solubility observed thus far, yielding a solubility of 41 g/L at 100°C.

The density lines (Table 16b, Figure 37) show the effects of substantial $PbCl_2$ solubility increases with increasing $MgCl_2$ additions (i.e., wide spacings). The increased $PbCl_2$ solubilities are also reflected by less negative slopes at the higher $MgCl_2$ concentrations (see Table 16b).

The logarithmic solubility lines (Table 16c, Figure 38) are also well-behaved. The calculated heats of solution decrease monotonically with increasing $MgCl_2$ levels (Table 17). The $PbCl_2$ isotherms were generated using a quadratic equation (disregarding the common ion effect terms in Equation 8), as shown in Table 18 and Figure 39. The three dimensional $PbCl_2$ solubilty surface (Figure 40) is of similar shape to the one shown in Figure 27 for the 0.3 M $FeCl_3$ - HCl system. The surface is quite flat but steeply inclined towards high temperatures and $MgCl_2$ concentrations. The maximum $PbCl_2$ solubility was 41 g/L at 100°C and 2.2 M $MgCl_2$.

Table 16 - Solubility and density data as a function of temperature for the aqueous $PbCl_2$ - 1.0 M HCl - 0.1 M $FeCl_3$ - $MgCl_2$ system containing 0.5 to 2.2 M $MgCl_2$.

Conc. $MgCl_2$ (M)	Fitted Equation Parameters A	B	C	Correlation Coefficients
a) Solubility vs Temperature: $S = At \times e^{Bt} + C$				
0.5	0.02860	0.01790	0.5863	0.99828
1.0	0.04602	0.01471	0.8020	0.99551
1.5	0.09320	0.01135	0.8660	0.99694
2.2	0.19040	0.00695	2.8667	0.99652
b) Density vs Temperature: $d = At + B$				
0.5	-0.0002958	1.0806		0.99302
1.0	-0.0002618	1.1072		0.99557
1.5	-0.0001970	1.1526		0.94421
2.2	-0.0001736	1.1947		0.94213
c) Log Solubility vs 1/T: $\text{Log } s = A \times (1000/T) + B$				
0.5	-1.4881	4.1913		0.99744
1.0	-1.3554	3.8998		0.99325
1.5	-1.3241	3.9897		0.99250
2.2	-1.0333	3.3283		0.99618

d = density of saturated solution;
S = $PbCl_2$ solubility (g/L); s = $PbCl_2$ solubility (g/100 g solution);
t = temperature (20 to 100°C); T = absolute temperature (K).

Table 17 - Calculated $PbCl_2$ heats of solution in aqueous solutions containing 1.0 M HCl, 0.1 M $FeCl_3$, and different $MgCl_2$ concentrations.

$MgCl_2$ (M)	0.0	0.5	1.0	1.5	2.2
$\Delta H_{Sol'n}$ (kJ/mol)	30.5	28.6	26.0	25.5	19.8

Table 18 - Solubility data as a function of $MgCl_2$ concentration (g/L) for the aqueous $PbCl_2$ - 1 M HCl - 0.1 M $FeCl_3$ system at selected temperatures between 20 and 100°C.

Temp. (°C)	Fitted Equation Parameters* A	B	C x 10^4	D x 10^2	E	Correlation Coefficients
20	-	-	2.3557	-2.5075	2.1230	0.99872
30	-	-	2.8212	-2.4394	2.6120	0.99974
40	-	-	3.2480	-2.1756	3.2355	1.00000
50	-	-	3.6176	-1.6922	4.0359	0.99989
60	-	-	3.9175	-0.9685	5.0947	0.99954
70	-	-	4.1327	0.0005	6.5058	0.99896
80	-	-	4.2445	1.2192	8.3916	0.99814
90	-	-	4.2438	2.6522	10.9230	0.99699
100	-	-	4.1220	4.2441	14.3160	0.99535

*see Equation 8: $S_t = A/c^2 + Bc + Cc^2 + Dc + E$ (g/L).

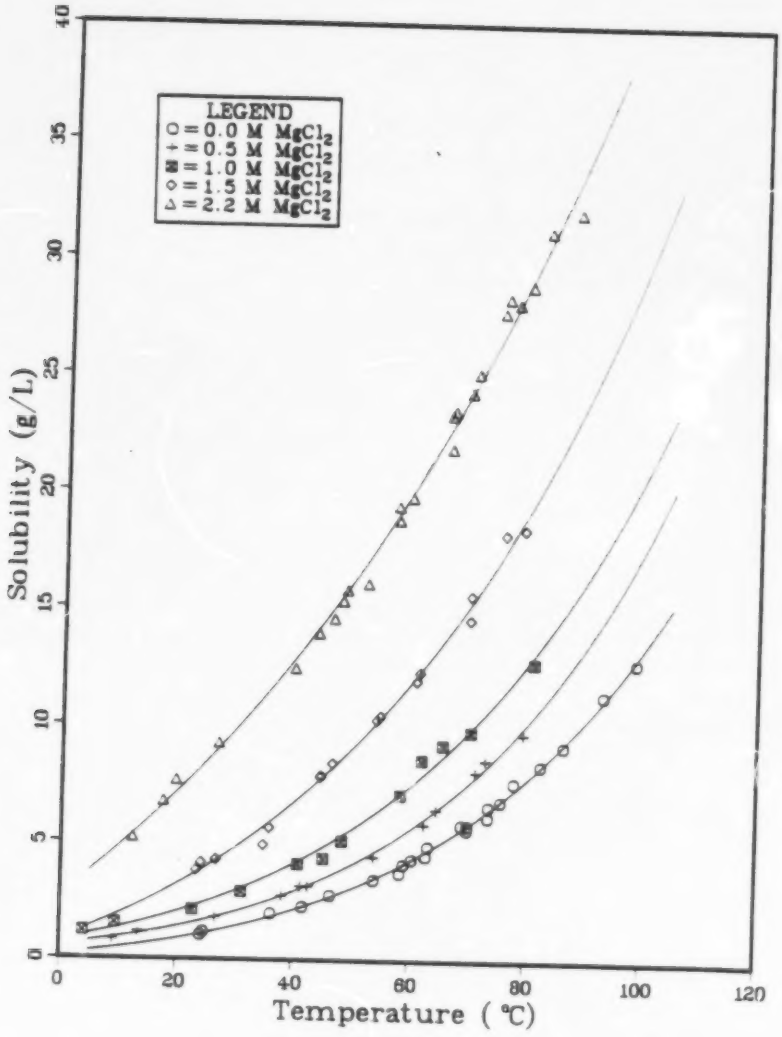

Fig. 36 - Solubility of $PbCl_2$ as a function of temperature for aqueous solutions containing 1.0 M HCl, 0.1 M $FeCl_3$ and 0.0 to 2.2 M $MgCl_2$.

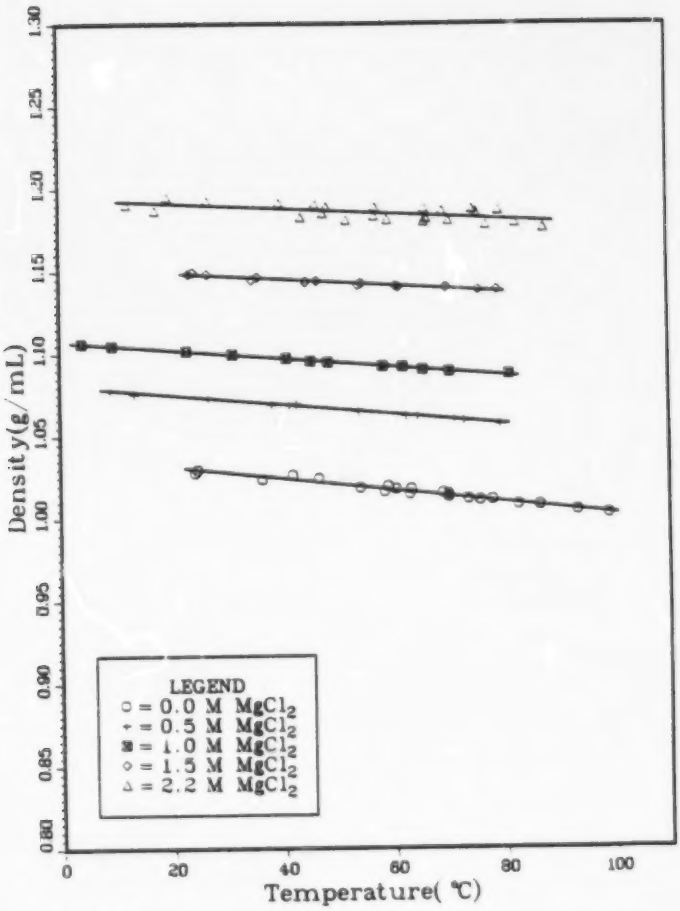

Fig. 37 - Density as a function of temperature for saturated solutions of $PbCl_2$ containing 1.0 M HCl, 0.1 M $FeCl_3$ and 0.0 to 2.2 M $MgCl_2$.

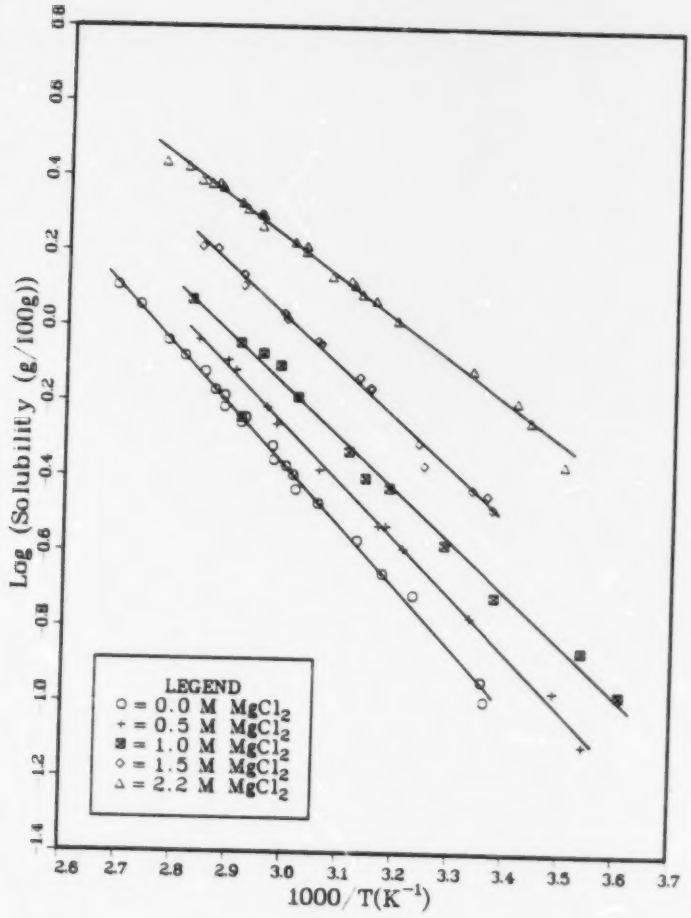

Fig. 38 - The logarithm of the $PbCl_2$ solubility as a function of the reciprocal of the absolute temperature for aqueous solutions containing 1.0 M HCl, 0.1 M $FeCl_3$ and 0.0 to 2.2 M $MgCl_2$.

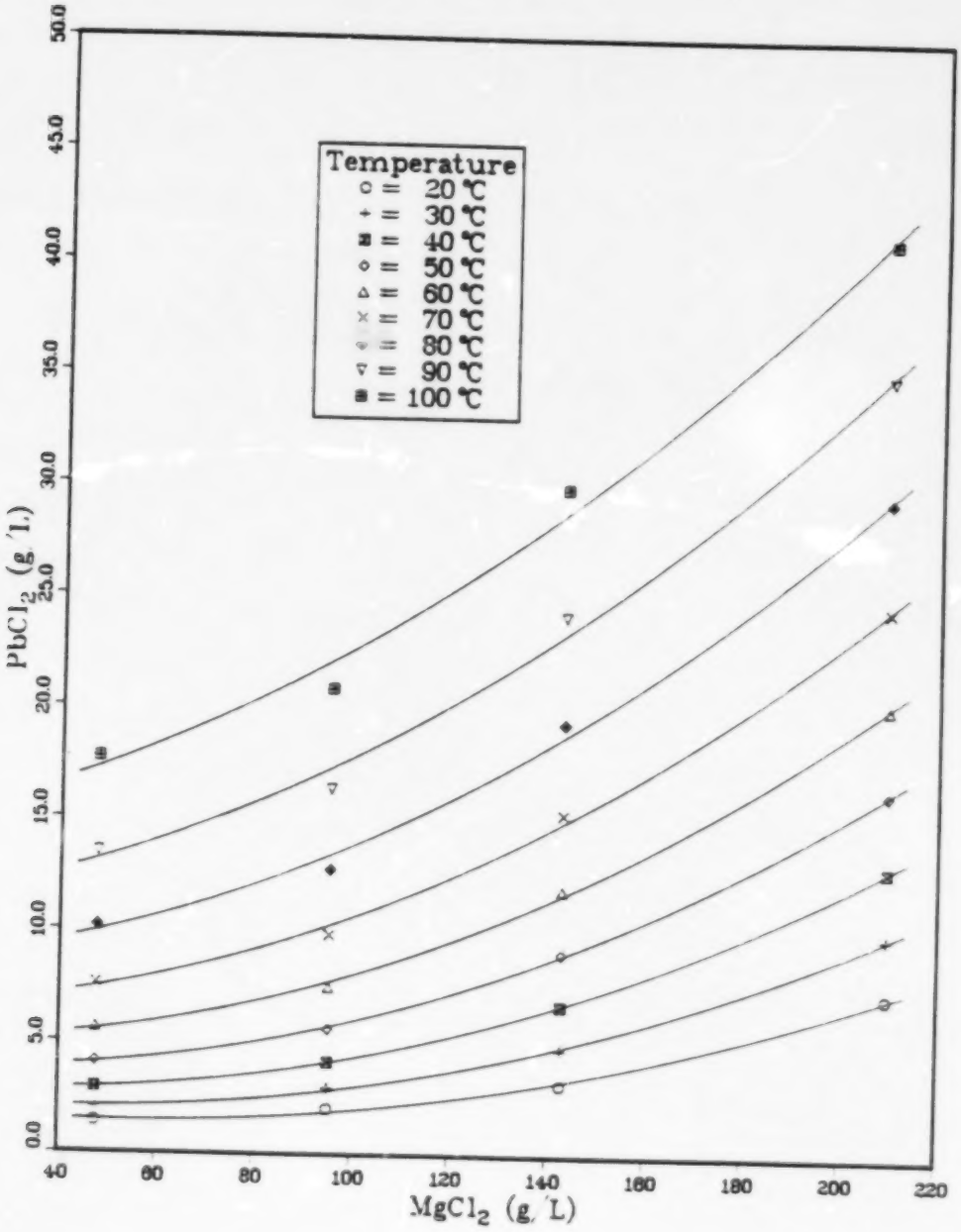

Fig. 39 - Solubility of $PbCl_2$ as a function of $MgCl_2$ concentration in 1.0 M HCl and 0.1 M $FeCl_3$, for selected temperatures between 20 and 100°C, as obtained from the 'best fit' parameters given in Table 18.

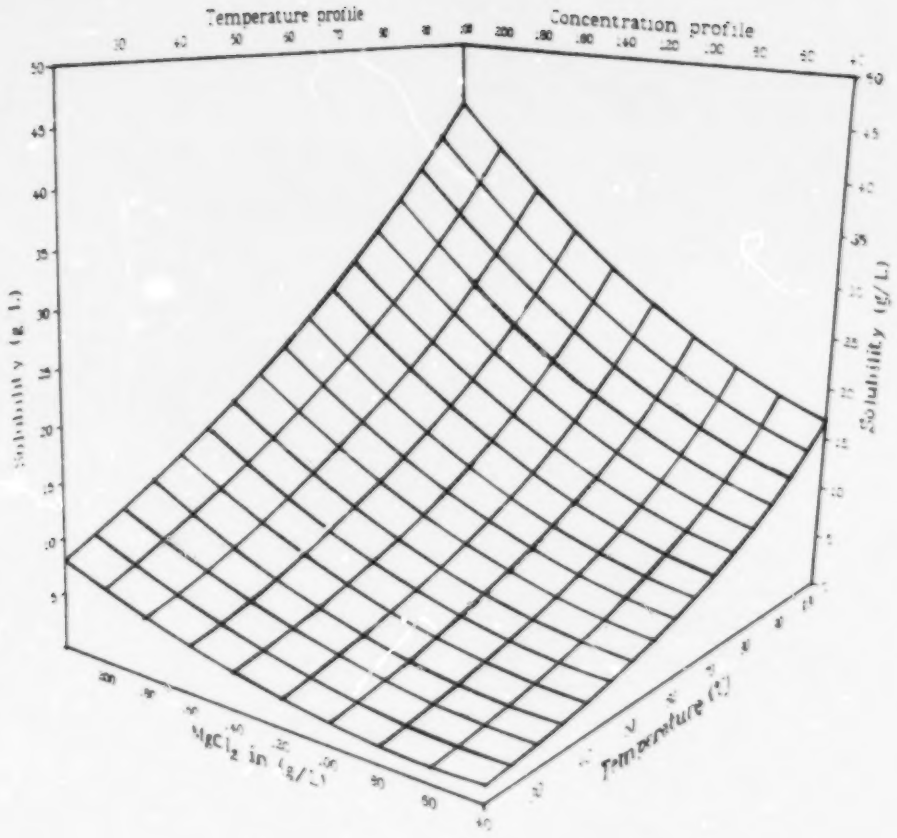

Fig. 40 - The $PbCl_2$ solubility 'surface' in 1.0 M HCl and 0.1 M $FeCl_3$ as a function of $MgCl_2$ concentration and temperature.

b) The Aqueous $PbCl_2$ - NaCl System

This section reports $PbCl_2$ solubilities in aqueous solutions containing 1.0, 2.0 and 3.0 M NaCl. The measurements are important as a basis for comparison with reported literature data, with $PbCl_2$ solubilities in aqueous HCl systems and with the aqueous $PbCl_2$-HCl-$FeCl_3$-NaCl systems of relevance to the CANMET ferric chloride leach process.

The $PbCl_2$ solubility curves (Table 19a, Figure 41) are spaced wider apart than the corresponding curves in the $PbCl_2$-HCl system (Figure 5). This is not surprising since NaCl is expected to dissociate to a much greater extent than HCl. Thus the 1.0 M NaCl solution is already well in the complexation region for $PbCl_2$, whereas a 1.0 M HCl solution is still in the transition region between the common ion effect and the complexation of $PbCl_2$. Furthermore, the $PbCl_2$ solubility in 3.0 M NaCl at 100°C is almost equal to the corresponding value in pure water (33 g/L at 100°C), whereas the maximum $PbCl_2$ solubility in the aqueous HCl system is only 18.1 g/L at 100°C in 3.0 M HCl.

The density lines of the $PbCl_2$-saturated NaCl solutions (Table 19b, Figure 42) are equidistant, reflecting the constant increment in free chloride ion with increased NaCl concentration. The decreasing negative slopes with increasing NaCl concentrations correspond to enhanced $PbCl_2$ solubilities due to complexation. As in the case of the aqueous $PbCl_2$-HCl system, the linear additivity rule is well obeyed.

The logarithmic solubility lines (Table 19c, Figure 43) are again well behaved. The calculated endothermic heats of solution (Table 20) decrease monotonically with increasing NaCl concentrations indicating a general correlation between solubilities and heats of solution. Isothermal solubility curves were not generated, but are expected to be qualitatively similar in behaviour to the curves in Figure 39 ($MgCl_2$ system).

A comparison with previously published solubility data in the $NaCl-H_2O$ system is given in Table 21. With only a few exceptions, the agreement between the measured and referenced values is within 5%.

Table 19 - Solubility and density data as a function of temperature for the aqueous $PbCl_2$ - NaCl system containing 1.0 to 3.0 M NaCl.

Conc. NaCl (M)	Fitted Equation Parameters A	B	C	Correlation Coefficients
a) Solubility vs Temperature: $S = At \times e^{Bt} + C$				
1.0	0.0471	0.01193	0.0126	0.99883
2.0	0.0628	0.01207	0.4878	0.99546
3.0	0.1173	0.00979	0.5972	0.99588
b) Density vs Temperature: $d = At + B$				
1.0	-0.0004163	1.0502		0.96500
2.0	-0.0003347	1.0818		0.87364
3.0	-0.0001596	1.1107		0.52435
c) Log Solubility vs 1/T: $\text{Log } s = A \times (1000/T) + B$				
1.0	-1.4392	4.0611		0.99447
2.0	-1.3487	3.9283		0.99179
3.0	-1.2808	3.9084		0.99540

d = density of saturated solution (g/mL);
S = $PbCl_2$ solubility (g/L); s = $PbCl_2$ solubility (g/100 g solution);
t = temperature (20 to 100°C); T = absolute temperature (K).

Table 20 - Calculated $PbCl_2$ heats of solution in various NaCl solutions.

NaCl (M)	1.0	2.0	3.0
$\Delta H_{Sol'n}$ (kJ/mol)	27.6	25.9	24.6

Table 21 - A comparison of measured solubility data for the aqueous $PbCl_2$ - NaCl system with selected literature values.

Conc. NaCl	Temp. (°C)	$PbCl_2$ Solubilities Literature	This work	% Diff.	Reference
1.02 M	25.0	1.75 M	1.65 M	-5	Herz &
2.05 "	"	2.67 "	2.60 "	-3	Hellebrandt (25)
3.03 "	"	3.55 "	4.20 "	+18	"
1.0 "	"	1.75 "	1.65 "	-6	Kendall &
2.0 "	"	2.60 "	2.60 "	--	Sloan (17)
3.0 "	"	4.25 "	4.20 "	-1	"
1.0 "	"	1.60 "	1.65 "	+3	Deacon (26)
1.0 g/kg	"	1.78 g/kg	1.71 g/kg	-4	Lewin, Vance &
2.0 "	"	2.74 "	2.78 "	+2	Nelson (27)
2.0 M	50.0	6.5 g/L	6.2 "	-5	Demassieux (28)
1.0 "	100.0	16.62 "	15.5 "	-7	"

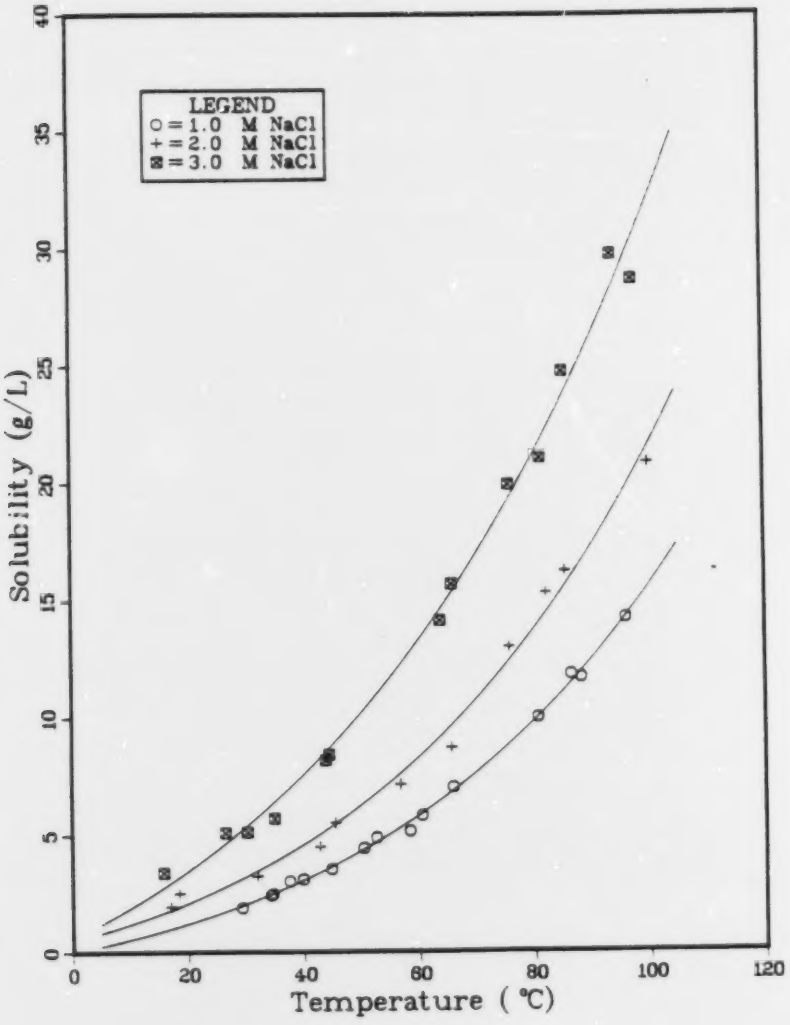

Fig. 41 - Solubility of $PbCl_2$ as a function of temperature for aqueous solutions containing 1.0, 2.0 and 3.0 M NaCl.

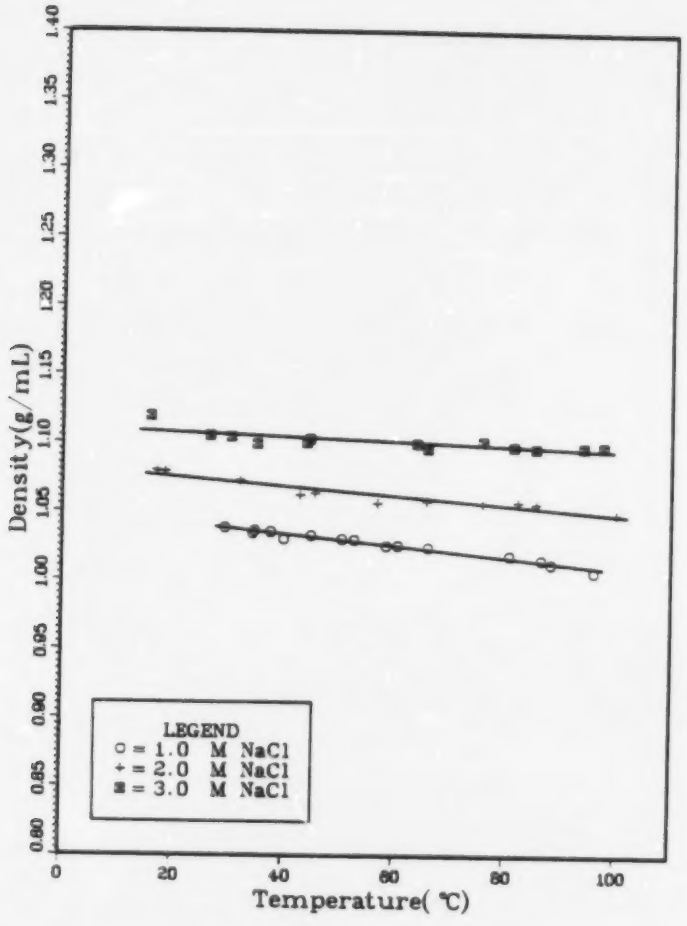

Fig. 42 - Density as a function of temperature for saturated solutions of $PbCl_2$ containing 1.0, 2.0 and 3.0 M NaCl.

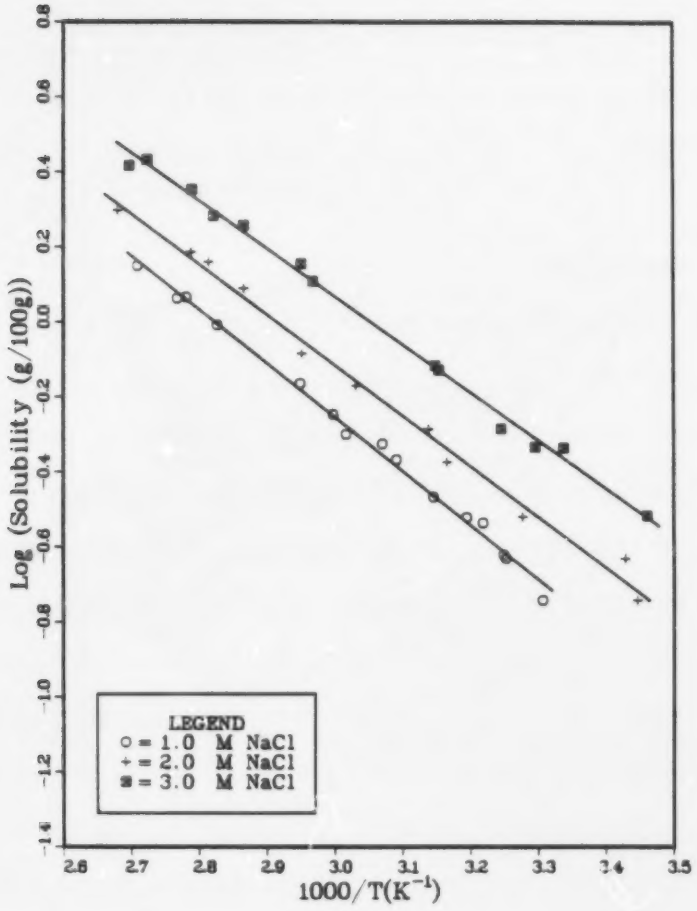

Fig. 43 - The logarithm of the $PbCl_2$ solubility as a function of the reciprocal of the absolute temperature for aqueous solutions containing 1.0, 2.0 and 3.0 M NaCl.

c) The Aqueous $PbCl_2$ - 1.0 M HCl - 0.1 M $FeCl_3$ - NaCl System

This section reports $PbCl_2$ solubilities in aqueous solutions of 1 M HCl and 0.1 M $FeCl_3$ containing 0.0, 0.5, 1.0, 2.0 and 3.0 M NaCl. The concentrated brines resemble those used in hydrometallurgical processes, and comparison of these results with previously discussed data completes this overview. Results of the solubility and density measurements are given in Figures 44 and 45, respectively. Calculated values of log s vs 1/T are presented in Figure 46. Results of the fitted parametric solubility equations in Figure 44 are summarized in Table 22. Calculated heats of solution are given in Table 23.

The $PbCl_2$ solubility curves (Table 22a, Figure 44) start off in the transition region (1.0 M HCl - 0.1 M $FeCl_3$ - 0 M NaCl), and are best compared to those for the corresponding $MgCl_2$-containing system (Table 16a, Figure 36). The initial effect of increasing NaCl levels from 0 to 0.5 to 1.0 M appears to be about half the corresponding increase observed for $MgCl_2$ additions. This indicates that both NaCl and $MgCl_2$ are dissociated to a similar degree at low total Cl^- concentrations. The 2.0 M NaCl curve, however, is already significantly higher than the 1.5 M $MgCl_2$, whereas the 3.0 M NaCl curve exceeds the 2.2 M $MgCl_2$ solubility curve. Since the maximum chloride contribution ratio of $MgCl_2$:NaCl is 2:1, and because the $MgCl_2$:NaCl concentration ratios in the above comparisons are only 1.33:1 and 0.73:1, respectively, it may be concluded that NaCl is sigificantly more dissociated than $MgCl_2$ at high total Cl levels. Thus, the maximum $PbCl_2$ solubility observed in the current study is 47.4 g/L at 100°C in aqueous 1.0 M HCl - 0.1 M $FeCl_3$ - 3.0 M NaCl. Judging from the effect of $FeCl_3$ on the $PbCl_2$ solubility shown in Figure 33, the $PbCl_2$ solubility in pregnant leach solutions typically containing 0.5 M HCl - 0.1 M $FeCl_3$ - 1.0 M $FeCl_2$ - 3.0 M NaCl (29) may well exceed the 60 g/L level at 100°C.

The density lines of $PbCl_2$-saturated solutions (Table 22b, Figure 45) are well behaved considering the complexity of the systems. This is probably related to the fact that the $FeCl_3$ concentration is low and the measurements are generally well inside the complexation region (compared to the aqueous $PbCl_2$ - $FeCl_3$ - HCl system). The $PbCl_2$ - 0.1 M $FeCl_3$ - 1 M HCl - $MgCl_2$ system is even better behaved for the same reasons. Thus, the variations of the slopes in Table 22b and Figure 45 cannot be completely rationalized in terms of increasing $PbCl_2$ solubilities, although preliminary calculations of the linear additivity contribution appear to be quite consistent.

Similar observations apply to the behaviour of the logarithmic solubility lines (Table 22c, Figure 46) and the calculated heats of solution (Table 23). The latter are somewhat more endothermic than those for the corresponding $MgCl_2$ levels (Table 17) even though the $PbCl_2$ solubility was highest in the presence of 3 M NaCl. By the same token, the heats of solution in the corresponding iron chloride systems (Tables 12 and 15) are less endothermic although the $PbCl_2$ solubilities are quite depressed. It may be argued, therefore, that the correlation between increasing $PbCl_2$ solubilities and less endothermic heats of solution is strictly applicable only within a particular co-electrolyte system where changes in the heats of formation of possible complexed species are limited. Different co-electrolytes in a particular order (e.g., NaCl, $MgCl_2$, $FeCl_2$, $FeCl_3$) will generally be associated with more exothermic heats of complexation. Since the heats of solution in these systems are the sum of various parts such as lattice energy, heats of hydration and heats of complexation, they will also become more exothermic in the same order. Complexation of the co-electrolytes, on the other hand, will withdraw free Cl^- ions available for complexation of the lead so that the $PbCl_2$ solubility will be reduced.

The solubility isotherms (Table 24 and Figure 47) were generated using a quadratic equation, in analogy to the corresponding $MgCl_2$ system (p.73). The solubility surface (Figure 48) is even more steeply inclined than in the $MgCl_2$ system (Figure 40), and the highest $PbCl_2$ solubility was observed to be about 48 g/L at 100°C and 3.0 M NaCl. This again indicates that NaCl is dissociated to a much larger extent than $MgCl_2$, and that the 0.1 M $FeCl_3$ concentration had no pronounced effect on the $PbCl_2$ solubility.

The above considerations suggest that the measured $PbCl_2$ solubilities are a sensitive indicator of available free Cl^- concentrations provided by the co-electrolytes in the solution. It should be interesting, therefore, to plot the isothermal $PbCl_2$ solubilities as a function of total added chloride concentrations and to compare the results for various co-electrolyte systems. Such isothermal plots at 25 and 100°C are given in Figures 49 and 50 with the total Cl concentration arbitrarily represented on a logarithmic scale to accentuate its effect on the $PbCl_2$ solubility. Both figures are similar, the major difference being the higher $PbCl_2$ solubilities and the anomalous effect of high $FeCl_3$ concentrations at 100°C.

At 25°C (Figure 49), the common ion effect region is generally encountered below total chloride concentrations of 1 M Cl^- (log = 0). In this region, only two aqueous systems were measured, namely $PbCl_2$ - HCl and $PbCl_2$ - 0.1 M $FeCl_3$ - HCl. Since $PbCl_2$ solubilities in the latter system seem to be slightly higher, 0.1 M $FeCl_3$ must be dissociated to a lesser extent than HCl at low Cl^- concentrations (free Cl^- depresses the solubility). In the transition and complexation regions above 1 M total chloride (log > 0), free Cl^- ions will improve the $PbCl_2$ solubility. Thus, the location of the curves indicates increasing Cl^- donor capacities at high total chloride levels in the order: $FeCl_3$ < HCl < $FeCl_2$ < $MgCl_2$ < NaCl.

Similar behaviour is observed at higher temperatures, including the results at 100°C represented in Figure 50 where the differences are more pronounced. The minimum $PbCl_2$ solubility corresponding to the transition from common ion effect to the complexation region is also found near 1 M total chloride (log = 0), and a finer distinction can be made for free Cl^- donors above this level: 1 M $FeCl_3$ < 0.3 M $FeCl_3$ < HCl < 0.1 M $FeCl_3$. It may also be surmised that the behaviour of a typical pregnant process solution containing very little $FeCl_3$ and HCl, but higher amounts of $FeCl_2$ and NaCl, will follow the curve for the $MgCl_2$-containing system quite closely, resulting in high $PbCl_2$ solubilities at high temperatures and high total chloride concentrations. Furthermore, regeneration of the ferric chloride (e.g., by chlorination) prior to $PbCl_2$ crystallization may improve the $PbCl_2$ recovery yields by depressing the $PbCl_2$ solubility in the mother liquor. Alernatively, $PbCl_2$ crystallization may occur during regeneration of raffinate saturated with $PbCl_2$ if the $PbCl_2$ recovery step precedes the oxidation.

Table 22 - Solubility and density data as a function of temperature for the aqueous $PbCl_2$ - 1.0 M HCl - 0.1 M $FeCl_3$ - NaCl system containing 0.5 to 3.0 M NaCl.

Conc. NaCl (M)	Fitted Equation Parameters A	B	C	Correlation Coefficients
a) Solubility vs Temperature: $S = At \times e^{Bt} + C$				
0.5	0.04360	0.01258	0.0701	0.99827
1.0	0.04019	0.01553	0.6358	0.99885
2.0	0.06367	0.01525	1.4321	0.99916
3.0	0.1396	0.01155	3.0558	0.99847
b) Density vs Temperature: $d = At + B$				
0.5	-0.0003444	1.0604		0.97961
1.0	-0.0003486	1.0780		0.89482
2.0	-0.0003444	1.1218		0.98837
3.0	-0.0002109	1.1502		0.94483
c) Log Solubility vs 1/T: $\text{Log } s = A \times (1000/T) + B$				
0.5	-1.6134	4.5650		0.99481
1.0	-1.4362	4.1143		0.99863
2.0	-1.3483	4.0486		0.99779
3.0	-1.1608	3.7255		0.99543

d = density of saturated solution (mg/L);
S = $PbCl_2$ solubility (g/L); s = $PbCl_2$ solubility (g/100 g solution);
t = temperature (20 to 100°C); T = absolute temperature (K).

Table 23 - Calculated $PbCl_2$ heats of solution in aqueous solutions containing 1.0 M HCl and 0.1 M $FeCl_3$ at different NaCl concentrations.

NaCl (M)	0.0	0.5	1.0	2.0	3.0
$\Delta H_{Sol'n}$ (kJ/mol)	30.5	31.0	27.6	25.9	22.3

Table 24 - Solubility data as a function of NaCl concentration (g/L) for the aqueous $PbCl_2$ - 1.0 M HCl - 0.1 M $FeCl_3$ - NaCl system at selected temperatures between 20 and 100°C.

Temp. (°C)	Fitted Equation Parameters* A	B	C x 10^4	D x 10^2	E	Correlation Coefficients
20	-	-	2.268	-1.043	1.395	0.99850
30	-	-	3.163	-1.772	2.325	0.99897
40	-	-	4.096	-2.344	3.397	0.99928
50	-	-	5.034	-2.648	4.618	0.99949
60	-	-	5.928	-2.540	5.992	0.99963
70	-	-	6.711	-1.829	7.520	0.99974
80	-	-	7.294	-0.269	9.197	0.99982
90	-	-	7.553	2.457	11.011	0.99987
100	-	-	7.334	6.752	12.294	0.99992

*see Equation 8: $S_t = A/c^2 + B/c + Cc^2 + Dc + E$ (g/L).

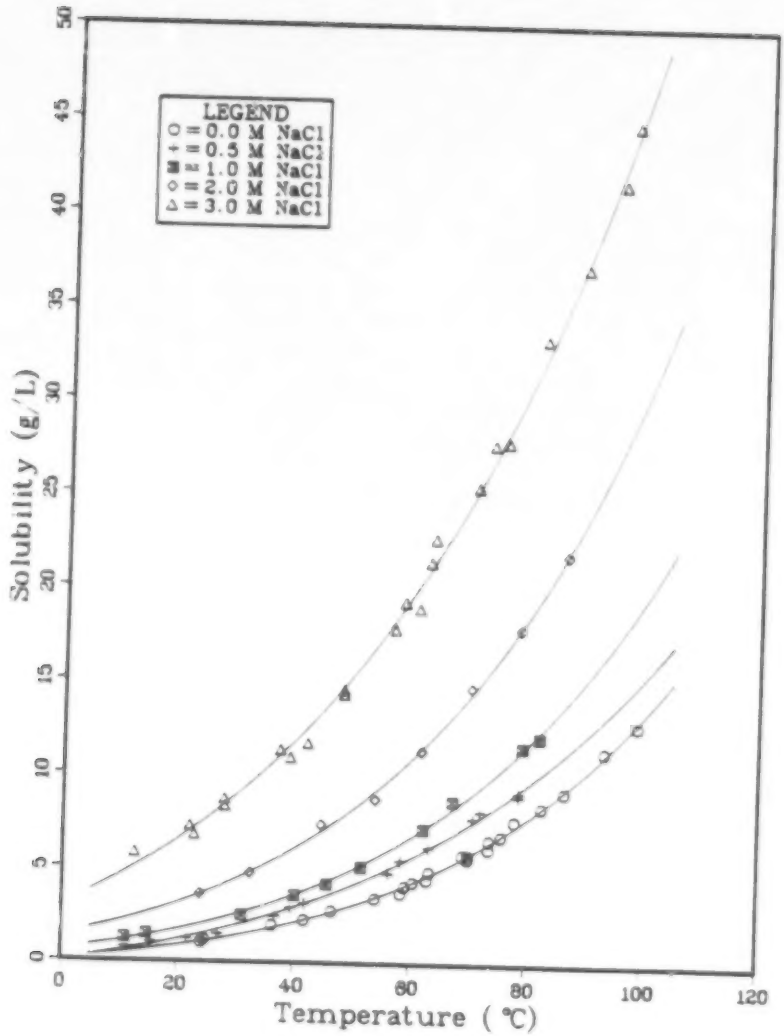

Fig. 44 - Solubility of $PbCl_2$ as a function of temperature for aqueous solutions containing 1.0 M HCl, 0.1 M $FeCl_3$ and 0.0 to 3.0 M NaCl.

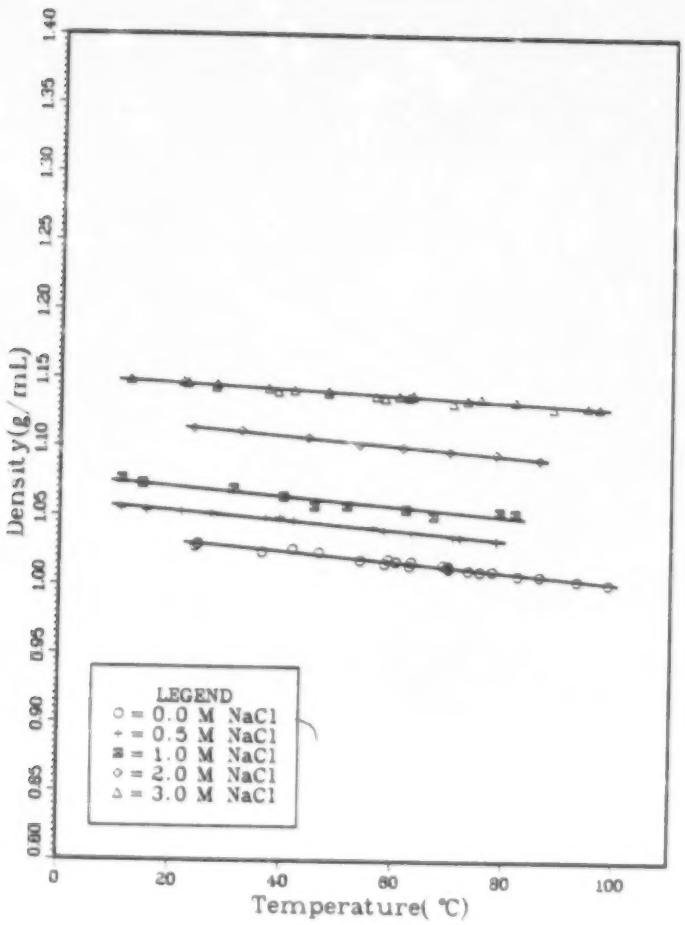

Fig. 45 - Density as a function of temperature for saturated solutions of $PbCl_2$ containing 1.0 M HCl, 0.1 M $FeCl_3$ and 0.0 to 3.0 M NaCl.

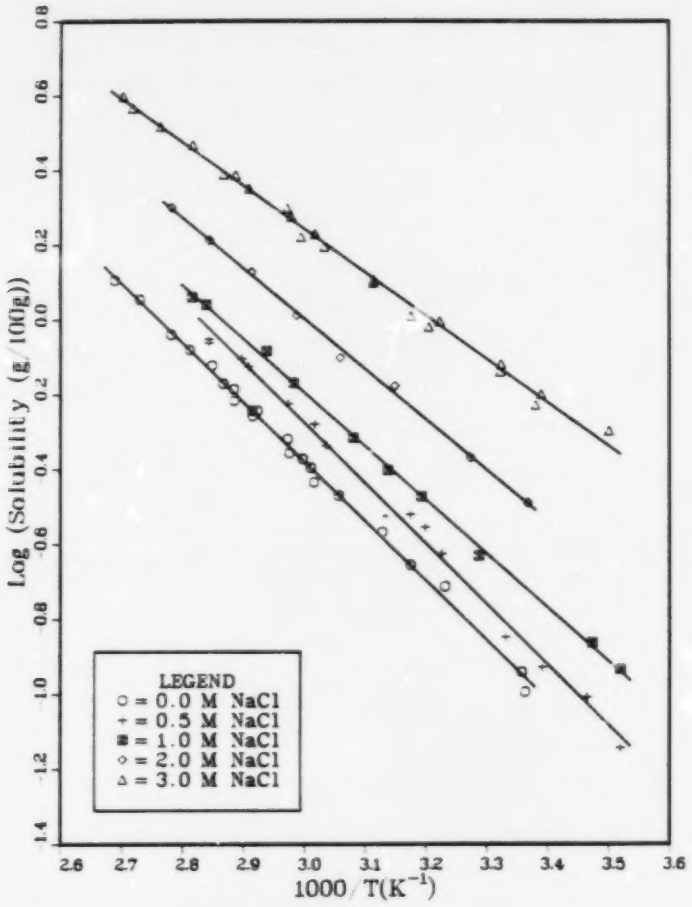

Fig. 46 - The logarithm of the $PbCl_2$ solubility as a function of the reciprocal of the absolute temperature for aqueous solutions containing 1.0 M HCl, 0.1 M $FeCl_3$ and 0.0 to 3.0 M NaCl.

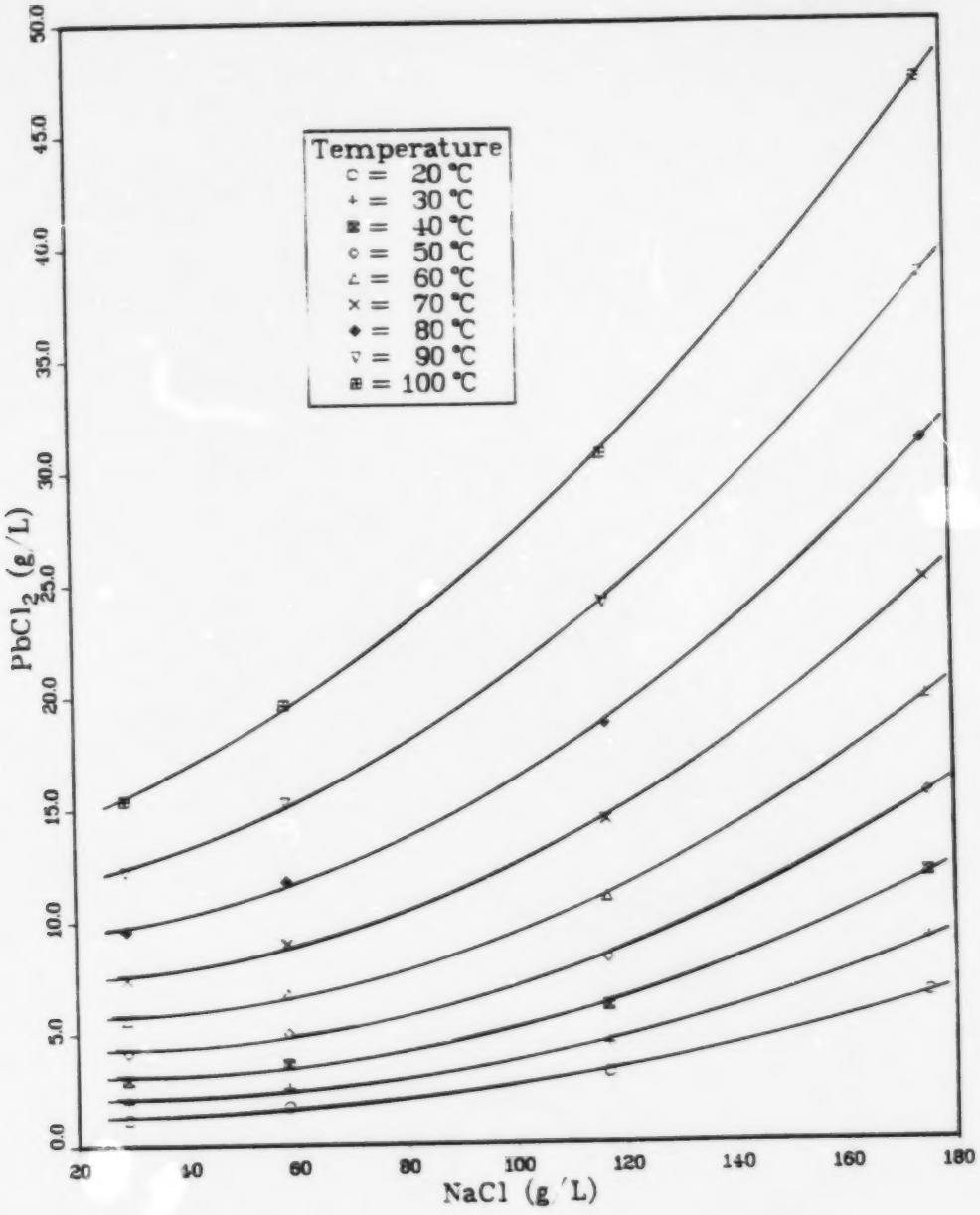

Fig. 47 - Solubility of $PbCl_2$ as a function of NaCl concentration in 1.0 M HCl and 0.1 M $FeCl_3$, for a selected number of temperatures between 20 and 100°C, as obtained from the 'best fit' parameters given in Table 24.

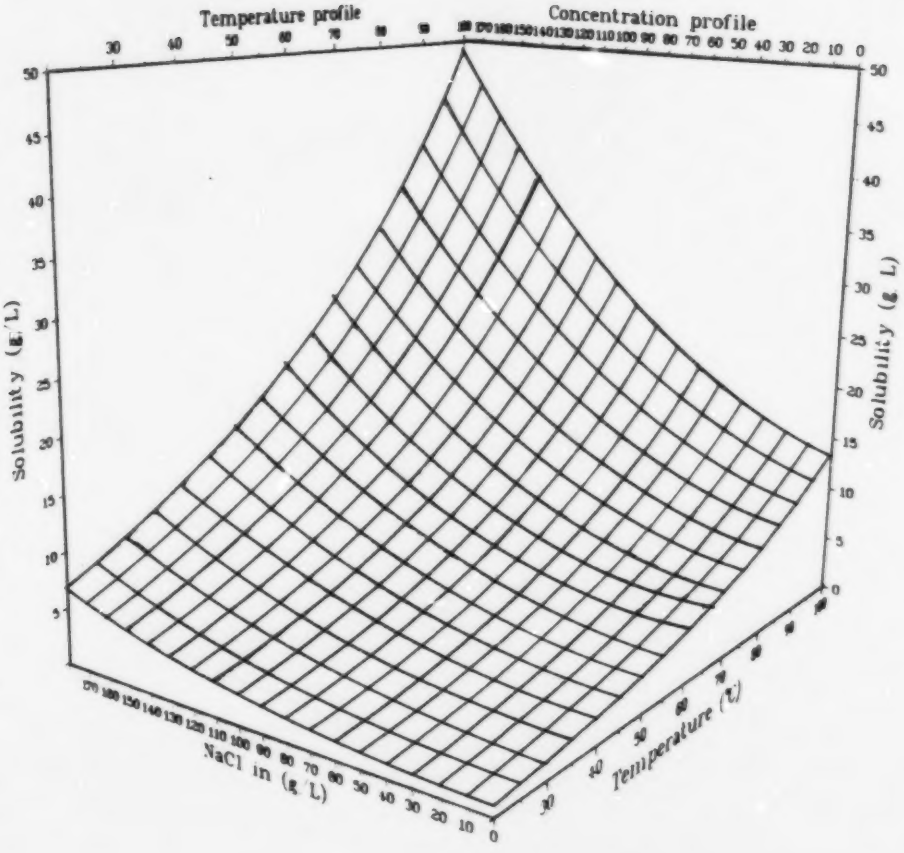

Fig. 48 - The $PbCl_2$ solubility 'surface' in 1.0 M HCl and 0.1 M $FeCl_3$, as a function of NaCl concentration and temperature.

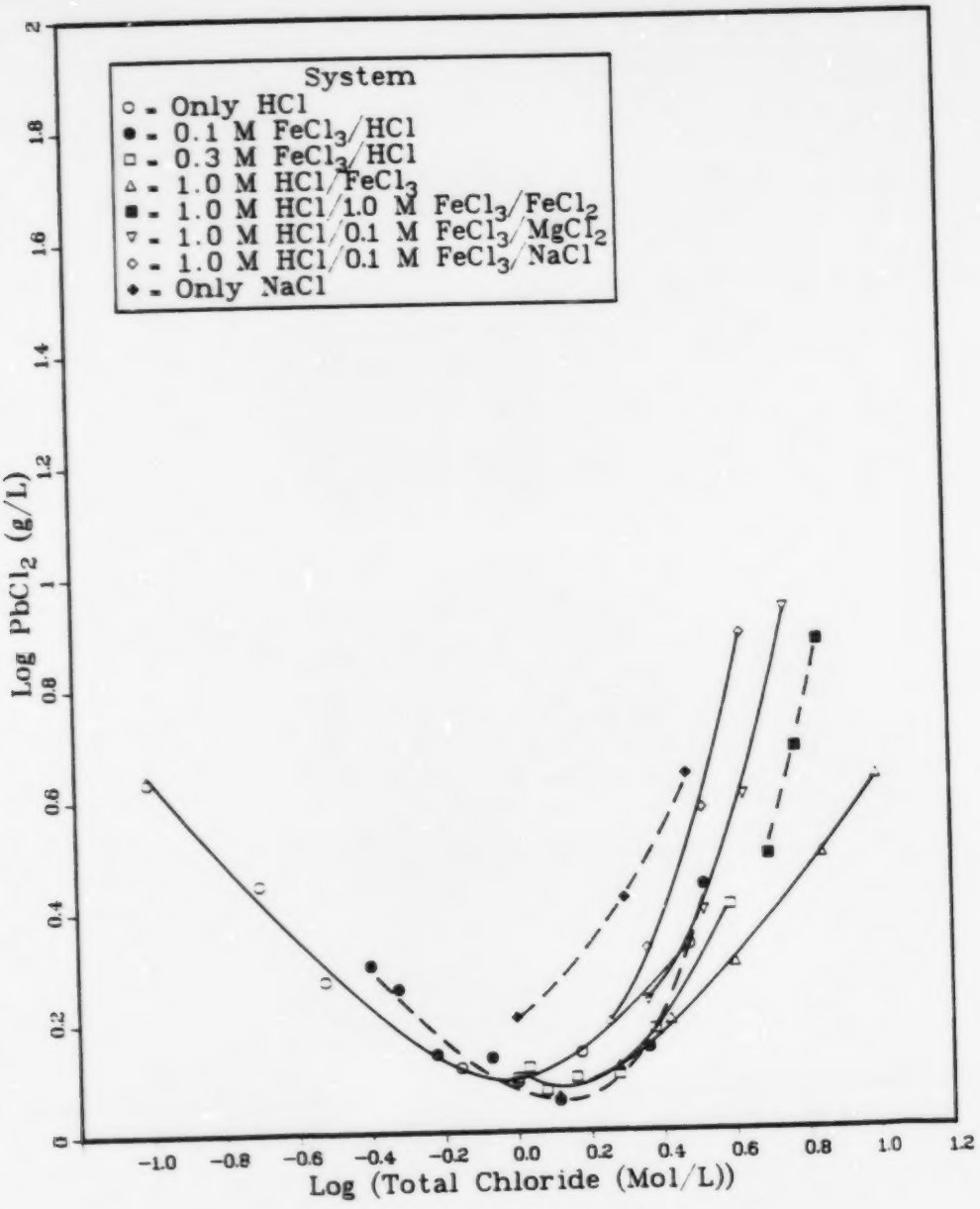

Fig. 49 - $PbCl_2$ solubility at 25°C as a function of the theoretically available total Cl^-, and assuming complete dissociation of the chloride salts in each base system.

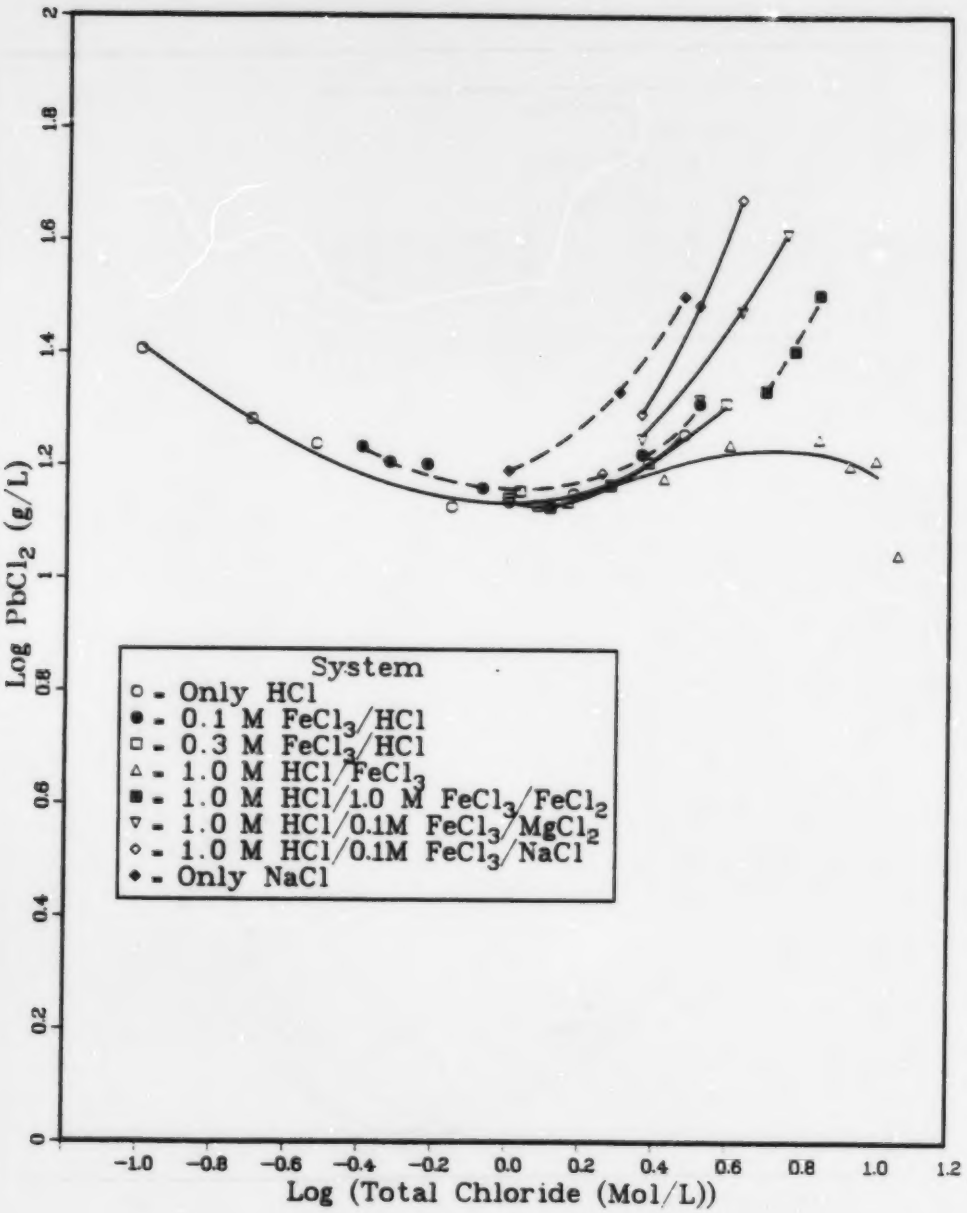
Log $PbCl_2$ (g/L)
Log (Total Chloride (Mol/L))
System
○ - Only HCl
● - 0.1 M $FeCl_3$/HCl
□ - 0.3 M $FeCl_3$/HCl
△ - 1.0 M HCl/$FeCl_3$
■ - 1.0 M HCl/1.0 M $FeCl_3$/$FeCl_2$
▽ - 1.0 M HCl/0.1M $FeCl_3$/$MgCl_2$
◇ - 1.0 M HCl/0.1M $FeCl_3$/NaCl
◆ - Only NaCl

Fig. 50 - $PbCl_2$ solubility at 100°C as a function of the theoretically available total Cl^-, and assuming complete dissociation of the chloride salts in each base system.

CONCLUSIONS

Solubility and density measurements have been carried out in the temperature range 20 to 100°C for various electrolyte solutions in equilibrium with excess $PbCl_2$ crystals. Isotonic and isothermal solubility curves, three-dimensional solubility surfaces, saturated solution density lines and isotonic heats of solution have been generated by fitting the experimental data points to empirical parametric equations. The pycnometric sampling method combined with the graphical representation techniques allowed a high accuracy and overall consistency to be obtained. The data, therefore, may be used for process design purposes, for future fundamental analysis, and as a basis for further studies.

A qualitative solubility model has been outlined in which trends and correlations between measured values and possible physical phenomena have been described in terms of the common ion effect, lead chloro complexation, co-electrolyte dissociation and complexation, and ionic saturation levels. More quantitative considerations should include derivation of activity coefficients and evaluation of stability constants as well as a molecular model for density contributions, solution structure, and thermodynamic calculations. This would require the precise identification and quantification of the existing dissolved entities by spectrophotometric or other physico-chemical means, including theorical calculations of solvent-solute interactions.

This report, therefore, is intended as a basis and a starting point for future efforts in this direction. With regards to practical applications, the effects of other co-electrolytes such as $ZnCl_2$, $CuCl_2$, silicates, sulphates, etc. may need additional investigation although relative trends may already be infered from these and related studies. Further refinements of the experimental and curve-fitting methods are also possible, and the ultimate

test of the procedures will be provided by a quantitative agreement between theory and measured data.

The anomalous $PbCl_2$ solubility behaviour in iron chloride-containing solutions will be investigated further. The plan is to examine first the region near 1.0 M HCl - 1.0 M $FeCl_3$ - 1.5 M $FeCl_2$ using a narrow grid of ferrous and ferric concentrations. A similar anomaly might be encountered in the $PbCl_2$ - 1.0 M HCl - 1.0M $FeCl_3$ - NaCl system which will be studied next. The final step would be a study of the $PbCl_2$ - 1.0 M HCl - 3.0 M NaCl - $FeCl_3$ - $FeCl_2$ system which resembles the expected process leach solutions most closely. Additional clues concerning the complexation behaviour of iron chlorides in concentrated brines should also be sought by spectroscopic methods and using solution X-ray, osmotic pressure, density and partial molal volumes, and activity coefficient measuring/calculation techniques. It is expected that further efforts in this direction will be rewarding, both from a fundamental and a practical point of view.

ACKNOWLEDGEMENTS

The authors wish to thank J. E. Dutrizac for helpful suggestions, and O. Dinardo for confirmatory measurements. Thanks are also due to R. F. Pilgrim for assistance in applying the 'Simplex' method.

REFERENCES

1. Dutrizac, J. E. "The Chloride Processing of Lead Concentrate"; Division Report MRP/MSL 84-41(LS); CANMET, Energy, Mines and Resources Canada; 1984.

2. Dinardo, O. and Dutrizac, J. E. "The Solubility of Silver Chloride in Ferric Chloride Leaching Media"; Hydrometallurgy 13:3:345-363; 1985.

3. Bartels, K. "Solubility of $PbCl_2$ in Hydrometallurgical Solutions: I. A Compilation of Published Data for $PbCl_2$ in H_2O"; Division Report MRP/MSL 80-77(TR); CANMET, Energy, Mines and Resources Canada; 1980.

4. Bicknell, T. L. and Bartels, K. "Solubility of $PbCl_2$ in Hydrometallurgical Solutions: II. Solubility Estimates of $PbCl_2$ in $FeCl_3$-HCl-H_2O and $FeCl_2$-HCl-H_2O Systems"; Division Report MRP/MSL 80-117(TR); CANMET, Energy, Mines and Resources Canada; 1980.

5. Clever, L. H. and Johnston, F. L. "The Solubility of Some Sparingly Soluble Salts: An Evaluation of the Solubility in Water and Aqueous Electrolyte Solution"; Reprint No. 166; J Phys and Chem Ref Data 9:3:751-784; 1980.

6. Nriagu, J. O. and Anderson, G. M. "Stability of the Lead(II) Chloride Complexes at Elevated Temperatures"; Chem Geol 7:171-183; 1971.

7. Mironov, V. E., Kul'ba, F. Ya., Fedorov V. A., and Fedorova, A. V. "Chloro-Complexes of Lead(II)"; Russ J Inorg Chem 9:9:1155-1156; 1964.

8. Federov, V. A., Kutuzova, M. Ya., and Mironov, V. E. "Chloride Complexes of Lead(II)"; Fiz Khim, Khim Tekhnol 1969:326-331; 1969.

9. "Handbook of Chemistry and Physics"; Weast, R. C. and Astle, M. J. editors; 60th ed; pp D227-276; Boca Raton, CRC Press Inc; 1979.

10. Garrels, R. M. and Christ, C. L. in "Solutions, Minerals and Equilibria"; Chapters 1 to 4; San Francisco, Freeman, Cooper and Co; 1965.

11. Lewin, T in "The Solubility Product Principle"; London, Sir Isaac Pitman & Sons, Ltd; 1960.

12. "Coordination Chemistry"; Martell, A. E. editor; Chapters 7 to 9; New York, Van Nostrand Reinhold Co; 1971.

13. Bockris, J. O'M. and Reddy, A. K. N. in "Modern Electrochemistry"; Vol. I; Chapters 2 and 3; New York, Plenum Press; 1970.

14. Brandes, D., Bedard, P. L. and Bartels, K. "Solubility of $PbCl_2$ in Hydrometallurgical Solutions: IV. Construction and Calibration of a Sampling Pycnometer in the Range 20°C to 95°C"; Division Report MRP/MSL 81-11(TR); CANMET, Energy, Mines and Resources Canada; 1981.

15. Olsson, D. M. and Nelson, L. S. "The Nedler-Mead Simplex Procedure for Function Minimization"; Technometrics 17:1:45-51; 1975.

16. Noyes, A. A. "Ueber die Bestimmung der Elektrischen Dissoziation von Salzen Mittels Loeslichkeits Versuchen"; Z Physik Chem 9:603-632; 1892.

17. Kendall, J. and Sloan,C. H. . "The Solubility of Slightly Soluble Chlorides in Concentrated Chloride Solutions"; J Am Chem Soc 47:2306-2317; 1925.

18. von Ende, C. L. "Ueber das Verhalten der Bleisalze in Loesungen"; Z Anorg Chem 26:129-166; 1901.

19. Wilkerson, L., Bathurst, N. O. and Parton, H. N. "Equilibria in Aqueous Lead Chloride Solutions"; Trans Farad Soc 33:623-628; 1937.

20. Bell, J. C. "On the Solubility and Crystallization of Plumbic Chloride in Water, and in Water Containing Various Percentages of Hydrochloric Acid, Specific Gravity 1.162"; J Chem Soc 21:350-355; 1868.

21. Creaser, C. S. and Creighton, J. A. "5-Coordinate Halogeno-Complexes and Related Ions: Halogeno-Complexes of Fe(III) and Ti(IV)"; J Inorg Nucl Chem 41:469-472; 1979.

22. Wertz, D. L. and Steele, M. L. "Coordination of Fe^{3+} in Concentrated Aqueous Solutions with Chloride Ligands", Inorg Chem 19:6:1652-1656; 1980.

23. Peters, E. in "Hydrometallurgy: Theory and Practice"; Course Notes, University of British Columbia; Chapter 2; 1985.

24. Dutrizac, J. E. "The Dissolution of Galena in Ferric Chloride Media", Metal Trans; (in press).

25. Herz, W. and Hellebrandt, M. "Die Loeslichkeit von Bleichlorid und Bleibromid in Waessrigen Loesungen von Alkali- und Erdalkalichlorid Salzen"; Z Anorg Chem 130:188-198; 1923.

26. Deacon, G. E. R. "Studies of Equilibria in the Systems Sodium Chloride-Lead Chloride-Water, Lithium Chloride-Lead Chloride-Water"; J Chem Soc 130:2063-2065; 1927.

27. Lewin, S. Z., Vance, J. E. and Nelson, L. B. "Solubility of Lead Chloride in Sodium Chloride, Perchloric Acid, and Hydrochloric Acid Solutions"; J Am Chem Soc 75:11:2768; 1953.

28. Damassieux, N. "Etude de l'Equilibre Entre le Chlorure et l'Iodure de Plomb et Quelques Chlorures et Iodures Alcalins en Solution Aqueuse"; Ann Chim 20:9:233-296; 1923.

29. Tan, K. G. and Bedard, P. L. 'The Development of a Miniplant Chlorinator for the Oxidation of Ferrous Chloride Solutions"; Division Report MRP/MSL 85-29(TR); CANMET, Energy, Mines and Resources Canada; 1985.